

EVALUATION OF TISSUE RESPONSE FROM THE REGENERATIVE MULTIELECTRODE
ARRAY (REMI) IMPLANT USING ATF-3 AND cJUN

by

SARITA BHETAWAL

Presented to the Faculty of the Graduate School of
The University of Texas at Arlington in Partial Fulfillment
of the Requirements
for the Degree of

MASTER OF SCIENCE IN BIOMEDICAL ENGINEERING

THE UNIVERSITY OF TEXAS AT ARLINGTON

December 2012

Copyright © by Sarita Bhetawal 2012

All Rights Reserved

ACKNOWLEDGEMENTS

I would like to express my greatest gratitude to my mentor, Dr. Mario Romero-Ortega for providing me with an opportunity to pursue research in the field of Neuroengineering. I am grateful to his patient guidance, enthusiastic encouragement and support throughout the course of study. I would also like to thank my committee members, Dr. Liping Tang and Dr. Young-Tae Kim for their support and help. I like to thank all my fellow lab mates, especially Dr. Jennifer Seifert, Dr. Collins Watson, Dr. Rafael Granja-vazquez, Vidhi Desai, Nivi Khobragade, Nilanjana Dutta, and Camilo Sanchez for their contribution to this research. I would like to thank my parents for their support and motivation throughout my entire college education

November 20, 2012

ABSTRACT

EVALUATION OF TISSUE RESPONSE FROM THE REGENERATIVE MULTIELECTRODE ARRAY (REMI) IMPLANT USING ATF-3 AND cJUN

Sarita Bhetawal M.S.

The University of Texas at Arlington, 2012

Supervising Professor: Mario I. Romero-Ortega

Currently available peripheral nerve regenerative interfaces such as the sieve and the micro-channel regenerative electrode, intended to be used for the control and natural feel from advanced robotic prosthetic devices, eventually fail due to nerve damage due to axonopathy. The Regenerative Multi-electrode array (REMI) developed in our lab overcomes this limitation by providing a non-obstructive pathway for regenerating axons. However, it is possible that the mismatch at the electrode-tissue interface may cause axonal injury during limb stretching. In order to determine if micro-motion at the REMI causes neuronal injury I evaluated the nuclear expression of Activating Transcription Factor 3 (ATF-3), and cJUN in the sensory dorsal root ganglia neurons, in animals that received either normal (70%) or excessive (100%) limb stretching. I hypothesized that persistent expression of ATF-3 would indicate continued micro-injuries caused by mechanical mismatch at the REMI electrode-nerve interface, and that cJun expression will decrease overtime, unless axonal regeneration is elicited by limb stretching. Sixteen adult rats received a REMI implant in the sciatic nerve and underwent weekly cyclical limb at 70% and 100% stretching (n=8 per group), and evaluated at 30 and 60 days. Quantitative analysis revealed that the percentage of ATF-3 expression decreased from 30 to

60 days in both 70% and 100% stretching groups, similarly to control animals, suggesting that REMI implantation does not cause micro-motion induced axonal injury. Conversely, the regenerative marker c-Jun showed an initial increment in expression, which was maintained for 60 days in the 70% stretch group, but reduced significantly at 60 days after 100% stretching. This unexpected finding may be explained by known beneficial effect of exercise in nerve regeneration. To determine if such response differs in the sub chronically injured nerves, c-Jun and ATF-3 expression was quantified in animals 30 days after nerve amputation. ATF-3 expression in this model showed a significant decrease from 15 to 60 days, comparable animals with acute REMI implantations. Together, the present results suggest that REMI implants do not induce tissue micro-injury and form a stable interface, supporting the notion that such interface might be reliably used to successfully interface the peripheral nerves with the intention to naturally control a robotic prosthetic device

TABLE OF CONTENTS

ACKNOWLEDGEMENTS	iii
ABSTRACT	iv
LIST OF ILLUSTRATIONS.....	ix
LIST OF TABLES	xiii
Chapter	Page
1. UPPER LIMB PROTHESES AND CONTROL MECHANISM	1
1.1 Prevalence of limb loss	1
1.2 Advancement in upper limb prostheses.....	1
1.3 Control Mechanism of Prostheses	3
1.3.1 Body powered prosthesis.....	3
1.3.2 Myoelectric prosthesis	4
1.3.3 Targeted Muscle Reinnervation	5
1.3.4 Cortical Interface	7
1.3.5 Peripheral nerve Interface.....	9
1.3.5.1 Extraneural electrode.....	10
1.3.5.2 Intraneural electrode.....	11
1.3.5.3 Regenerative electrode.....	13
2. PHERIPHERAL NERVE REGENERATION	16
2.1 Introduction.....	16
2.2 Neuronal changes occurring at injury site.....	17
2.3 Axonal Injury signals to soma	19
2.4 Gene regulation and transcriptional factors	21

2.4.1 Activating Transcriptional Factor 3 (ATF-3)	23
2.4.2 c-Jun.....	24
2.5 Current limitations	26
2.6 Specific aims of the project	27
2.4.1 Specific aim 1	27
2.4.2 Specific aim 2.....	27
3. SPECIFIC AIM 1	29
3.1 Micro-motion.....	29
3.2 Materials and Methods.....	31
3.2.1 Surgical and Implantation.....	32
3.2.2 Stretching	33
3.2.3 Extraction Dorsal Root Ganglia (DRG)	34
3.2.4 Sample preparation and Cryosectioning.....	34
3.2.5 Immunofluorescence staining	35
3.2.6 Image Analysis and Quantification.....	35
3.3 Results	36
3.3.1 Comparison between Nerve Stretching and No Stretching	42
3.4 Discussion.....	45
4. SPECIFIC AIM 2	48
4.1 Sub-Chronic Injury	48
4.2 Materials and Methods.....	49
4.2.1 Surgery and Implantation	50
4.3 Results	51
4.3.1 Comparison between Sub-Chronic Vs Acute.....	55
4.4 Discussion	57
5. CONCLUSION AND FUTURE WORK.....	59

REFERENCES.....	63
BIOGRAPHICAL INFORMATION	72

LIST OF ILLUSTRATIONS

Figure	Page
1.1 Upper limb prostheses: A) Mechanical Hooks, B) Mechanical Hands, D) Living Skin, E) DEKA arm	3
1.2 Body-powered prosthesis: The harness captures the user’s motion and transfer this movement through the cable to control the terminal devices	4
1.3 Myoelectric prosthesis: Myoelectric prosthesis: It uses the EMG signals, obtained from residual muscles, to operate the motorized terminal devices.....	5
1:4 Target muscles Reinnervation: In T5 patient, the distal radial nerve was transferred to the lateral triceps muscle, leaving the long head of the triceps to provide EMG signals for elbow extension whereas the median nerve was transferred to the medial biceps to provide EMG signals for elbow flexion.	6
1. 5 Cortical Interface: Tetraplegic , 58-year-old women using the robotic arm to grasp the bottle, bring it towards her mouth, drink coffee from the bottle through a straw and place the bottle back on the table using DLR robotic arm. Microelectrode was implanted 5.3 years before the beginning of this study.	8
1.6 Classification of peripheral nerve interface electrodes.	10
1.7 Extraneural electrodes: a) silicone and hybrid silicone-polyimide cuff electrode. B) FINE electrode.	11
1.8 Intraneural electrodes: A) polymer-based intrafascicular electrode (polyLIFE). B) Multielectrode Array from University of Utah. C) Utah slanted electrode array.	13
1.9 Regenerative electrodes: A) Sieve electrode B) Regenerative Multi-electrode Array	14
1.10 Classification of different types of peripheral nerve interface electrodes according to sensitivity and invasiveness.	15
2.1 Major events that occurred after injury: a) Wallerian degeneration, b) Propagation of injury signal to cell body, c) Activation of transcription factors via cascade of signaling pathway, d) Expression of regeneration associate genes (RAGs).	16
2.2 Regeneration process of Peripheral nervous system at the injury site:	18
2. 3 Injury signals propagate from injury site to cell body.	21
2.4 Activation of cascades of signaling pathways after peripheral injury:	23

2.5 Transcriptional regulation of regeneration associate gene, Damage-induced neuronal endopeptidase (DINE): Before injury, Transcriptional complex express DINE at low level. Following injury, injury-inducible transcriptional factor ATF3 form a heterodimer with c-Jun and Sp1 provides a platform to recruit ATF3, c-Jun, and Stat3 which express DINE at higher level.	24
2.6 Transcriptional factors, ATF-3 and c-Jun, expressed in minimum level but will activate in DRGs after sciatic nerve transection. c-Jun will be expressed throughout the nerve regeneration. As ATF-3 is the injury marker, it will express immediately after injury and will gradually decreased.	28
3.1 Tethered mode of implantation, (B) Untethered mode of implantation, (C) & (D) Tissue reaction after 12 weeks of Implantation; immunohistochemically labeled for GFAP (red), ED1 (green) and DAPI (blue).	30
3.2 Experimental design of specific aim 1: After sciatic nerve transection, REMI was implanted followed by either moderate or excessive limb stretching. After 30 days and 60 days time points, animals were perfused and L4-L5 DRGs were stained with c-Jun or AFT-3.	31
3.3 Surgery and Implantation: A) REMI Implantation after the transection of sciatic nerve. B) REMI was covered with the pedestal for external interface and was hold by the bone cement.	33
3.4 Limb stretching by using linear actuator and pelvic fixation device.	34
3.5 Negative staining control: Ipsilateral L4/L5 DRGs with secondary antibody but without primary antibody of ATF-3 and c-Jun to observe the effects of secondary antibody	37
3.6: Counterstaining with DAPI as a nuclear marker. Ipsilateral L4/L5 DRGs Staining with ATF-3 and c-Jun with DAPI to validate the positive nucleus staining of ATF-3 and c-Jun. Green: ATF-3, RED: c-Jun, Blue: DAPI. Arrow indicates the positive cells	38
3.7 Positive Staining control: Ipsilateral L4/L5 DRGs, 48 hours after sciatic nerve transection, were stained with ATF-3 and c-Jun. Arrow indicates the positively stained cells	38
3.8 Minimum expression of ATF-3 and c-Jun was observed in ipsilateral L4/L5 DRGs of uninjured animals.	39
3.9 ATF-3 expression in ipsilateral L5 /L4 DRG with either moderate or excessive Limb stretching at 30 days and 60 days after injury. Atf-3 expression decreased significantly from 30 days to 60 days but was comparable between moderate stretching and excessive stretching at 30 days and 60 days respectively. (n=4, p<0.05)	39
3.10 ATF-3 expression in ipsilateral L5 /L4 DRG decreased significantly with either moderate or excessive Limb stretching at 30 days and 60 days after injury respectively. (n=4, One way ANOVA: p<0.05)	40
3.11 c-Jun expression in ipsilateral L4/L5 DRG with either moderate or excessive Limb stretching at 30 days and 60 days after injury. c-Jun expression decreased significantly from 30 days to 60 days at 100% stretching. (n=4, p<0.05)	41

3.12 c-Jun expression in ipsilateral L4 /L5 DRG decreased significantly at 60 days after injury with 100% stretching. (n=4; One way ANOVA: P<0.05)	42
3.13 c-Jun expression in ipsilateral L5 /L4 DRG in acute injury without stretching at 15, 30 and 60 days after injury. ATF-3 and c-Jun expression was comparable between REMI implanted animals and control animals. Control animals were implanted with empty tube without REMI. c-Jun is in Red whereas ATF-3 is in green. (n=4; One way ANOVA: P<0.05) (Khobragade 2011)	43
3.14 ATF-3 expression in ipsilateral L5 /L4 DRG of Stretched animals (either moderate or excessive stretching) is not significantly different compared to unstretched animals. (n=4: One way ANOVA; p<0.05)	44
3.15 c-Jun expression in ipsilateral L5 /L4 DRG decreased significantly in excessive stretching animals compared to no stretching animals at 60 days after injury (n=4; One way ANOVA; p<0.05)	45
4.1. In the absence of distal segment, accumulations of growth cones undergo the formation of neuroma.....	49
4.2 Experimental design of sub chronic injury: Following the transection of sciatic nerve, proximal stump was sutured to the pectoral muscles. After a month, sciatic nerve was transected proximal to the first injury followed by REMI implantation. After 15 days, 30 days and 60 days of REMI implantation, animals were perfused and L4-L5 DRGs were stained with c-Jun or AFT-3.	50
4.3 Procedure of creating sub-chronic injury model. A) Sciatic nerve without the REMI implant. B) Sciatic Nerve is transected. C) Proximal stump of transected nerve is ligated to the biceps femoris muscles. D) Sciatic nerve undergoes second transection proximal to the first transaction and REMI was implanted.	51
4.4 Minimum expression of ATF-3 and c-Jun was observed in ipsilateral L4/L5 DRGs of uninjured animals.....	52
4.5 Atf-3 expression in ipsilateral L4/L5 DRGs in sub-chronic injury animals at 15 days, 30 days and 60 days. Arrows indicates the Atf-3 stained DRGs. Atf-3 decreased significantly from 15 days to 30 days to 60 days. (n=4, p<0.05)	53
4.6 The expression of ATF-3 in ipsilateral L5 /L4 DRGs decreased significantly from 15 days to 30 days to 60 days. (n=4, One way ANOVA; p<0.05)	53
4.7 c-Jun labeled L4/L5 ipsilateral DRGs at 15 days, 30 days and 60 days after sub-chronic injury. c-Jun expression decreased significantly from 30 days to 60 days (n=4, p, 0.05)	54
4.8 c-Jun expression in ipsilateral L5 /L4 DRG decreased significantly from 30 days to 60 days. (n=4; One way ANOVA; p <0.05)	54
4.9. The percentage of ATF-3 expression in ipsilateral L5 /L4 DRG of Sub-chronic injury is not significantly different compared to acute injury at 15 days, 30 days and 60 days respectively. (n=4; One way ANOVA; p<0.05)	56

4.10 .The percentage of c-Jun expression in ipsilateral L5 /L4 DRG of Sub-chronic injury increased significantly at 15 days and 30 days compared to acute injury. (n=4; One way ANOVA; p<0.05)57

LIST OF TABLES

Table	Page
1.1 Comparison between the Characteristics of the Different Human–Machine Interfaces for the Control of Hand Protheses in Amputees	9
2.1 Effects of Transcription factor c-Jun deletions and ATF-3 over expression on peripheral nerve regeneration	26
3.1: Dilution factors of primary and secondary antibodies for cJun and ATF3 staining.....	35

CHAPTER 1

UPPER LIMB PROTHESES AND CONTROL MECHANISM

1.1 Prevalence of Limb Loss

As of 2005, 1.6 million people have suffered from limb loss in the United States and the number is projected to double by the year 2050 (Ziegler-Graham et. al. 2008). Each year the number of limb amputation is estimated to increase by 185,000 due to disease and trauma (Owings et. al. 1998). The life-style of amputees as a result is heavily impacted in socio-economical aspects. Recently, robotic prostheses have been an area of research interest aiming to improve the quality of life for people with loss limb. The National Institutes of Health and the Defense Advanced Research Projects Agency (DARPA) have put their efforts in the development of reliable prostheses that can interface with the residual limb to control motor function and provide sensory feedback.

1.2 Advancement in upper limb prostheses

Upper limb prosthesis consists of two components, sockets and terminal devices (Behrend et. al. 2011). Sockets help to fit the terminal device to the patient's body. Terminal device is divided into two categories, passive and active. Passive terminal device include simple hook or cosmetic hand that has no moving function whereas active terminal device include functional moving hook, hand or specialized tools that perform various task such as grasping, holding or picking objects according to the users need (Behrend et. al. 2011). Terminal device has been significantly developed from mechanical hooks to robotic arms in order to provide equal or greater prehension as a human hand.

Currently used prosthetic hooks (Fig 1.1A) were originally developed in the early 1900 and have proven to be an effective and reliable tool for amputees. However, there are one or two moving parts in the entire system. It requires high gripping force when handling large or

heavy objects, which can result in muscle fatigue and pain (Billock et. al. 1986). Mechanical hands (Fig 1.1B) are heavy and unnatural for fine prehension activities as compared to mechanical hooks, which can provide 8-12 lbs of prehension, but at a slower response time (Billock et. al. 1986). However, mechanical hands offer very limited functionality such as closing and opening. Thus, current researches in upper-limb robotic prosthesis aim at developing robotic prosthesis that can provide full and realistic control. A human hand has complex kinematics with 23 degree of freedom and intrinsic sensory mechanisms (McLoughlin, 2009). Advanced robotic prosthetic hands with multiple degrees of freedom have been developed. Touch Bionics was the first company to commercialize one of these hands known as the iLimb (Fig 1.1C), which is comprised of articulating fingers including a thumb that enables the user to grasp and maneuver objects (Bandara et. al. 2012). More recently, Dean Kamen developed The Luke Arm, collaboration between Deka and the Applied Physics Laboratory at Johns Hopkins University funded by Defense Advanced Research Projects Agency (DARPA). The Deka arm (Fig 1.1D) provides 18 degrees of freedom and is adjustable so as to be used by anyone with any level of amputation (Bandara et. al. 2012, Neri et. al. 2008). Another DARPA funded project launched Proto 2 prosthetic, aims at fabricating a prosthetic arm populated with 100 sensors and connect the natural neural signals of body, providing sensory feedback loop (Bandara et. al. 2012). Moreover, researchers are working on improving sensory technology such as developing MEMs-based "smart-skin" (Gonenli et. al. 2011). Despite such progress in prosthetic devices, the technology and methods used for its control lag far behind. Even though the DEKA arm could provide 18 degree of freedom, providing the user of such prostheses with natural control and feel still remains a formidable challenge.

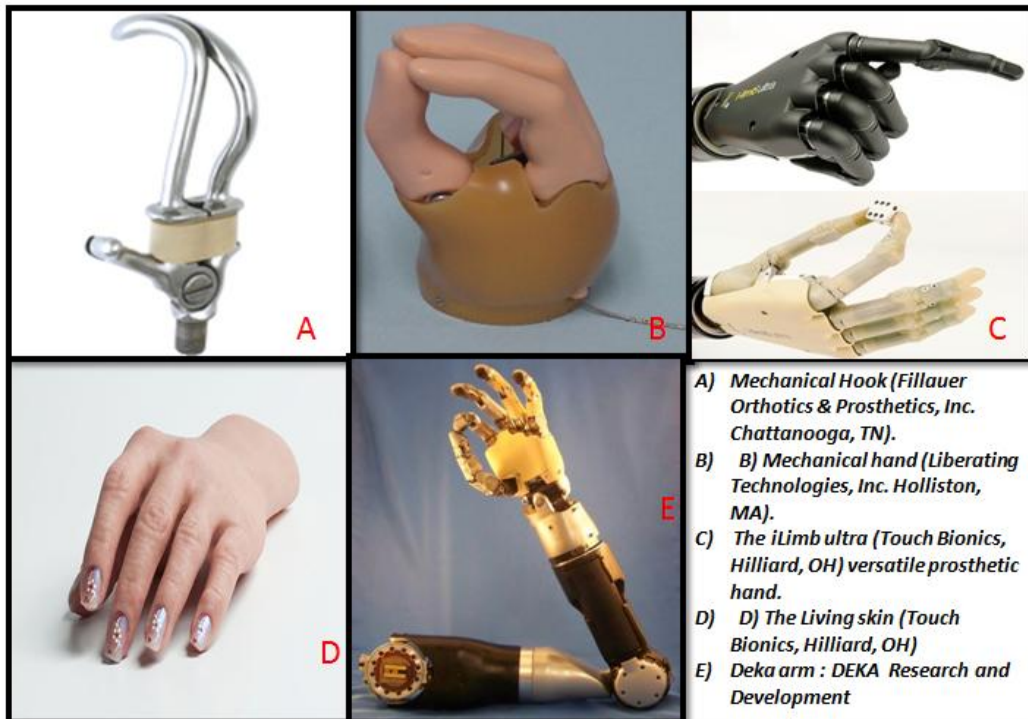


Figure 1.1 Upper limb prostheses. A) Mechanical Hooks; B) Mechanical hand; C) The ilimb Ultra; D) The Living skin; E) DEKA arm.

1.3 Control Mechanism of Prostheses

Many technologies have been either proposed or demonstrated to be capable of providing multiple degrees of freedom within a computer interface. Currently used methods, such as body powered and myoelectric control, and ongoing research on cortical interface and peripheral interface will be discussed here.

1.3.1 Body-powered prosthesis

Prior to the development of electrical arm, mechanical hands or hooks were actuated and controlled manually via utilizing the motion and gross force generated by body movement (Billock et. al. 1986). In this system, the amputee wears the harness that translates the shoulder motion into elbow flexion then a gravitational force generates the elbow extension (Doeringer et. al. 1995). Bowden cable control system is the common example that utilizes the force and

motion generated by the flexion-abduction movements at the glenohumeral joint to control the terminal device (Billock et. al. 1986).

Such control system requires a large amount of force since gross body movement controls entire system manually. Therefore, it possesses a limited range of motion such as closing and opening of terminal device (Behrend et. al. 2011, Doeringer et. al. 1995). Since Body powered prostheses are controlled manually with gross body movement, it cannot assist different levels of amputations.



Figure1.2 Body-powered prosthesis: The harness captures the user's motion and transfers this movement through the cable to control the terminal devices (Behrend et.al. 2011)

1.3.2 Myoelectric prosthesis

Myoelectric control system uses the electric signals obtained from the residual muscles to control the movement of terminal devices. Myoelectric signals are collected via surface electrode placed on the skin, then amplified, filtered, digitized using standard Electromyography (EMG) instrument and finally transferred to a controller (Oskoei et. al. 2007). This system is noninvasive and hands- free. It executes according to user intension thus, requiring less energy and providing more comfort as compared to the body-powered prostheses (Billock et. al. 1986)

However, myoelectric control system requires a sufficient amount of remnant muscle and nerve fibers to record the EMG signals (Behrend et. al. 2011). The residual muscles could provide physiologically unrelated movement that is not user intentional (Behrend et. al. 2011, Kuiken et. al. 2009). Since EMG signals are recorded at skin surface, the response time of

such control system is high. Even though, it provides wheelchair movement and grasping control, non-natural control strategies need to be learnt by the patient (Oskoei et. al. 2007, Micera et. al. 2012). Also, it lacks sensory feedback and is limited to providing only signal function control at a time (Behrend et. al. 2011).

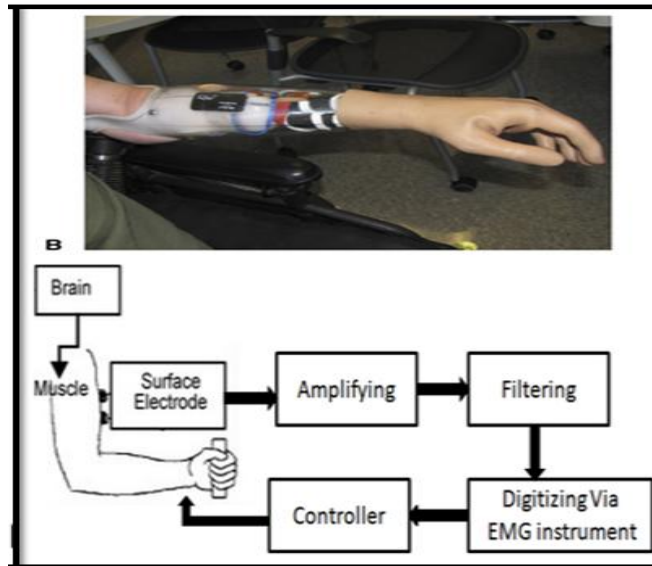


Figure 1.3 Myoelectric prosthesis: It uses the EMG signals, obtained from residual muscles, to operate the motorized terminal devices. Source: (Behrend et.al. 2011)

1.3.3 Targeted Muscle Reinnervation

To improve the EMG signals, Dr. Todd Kuiken and his collaborators developed a surgical technique known as Targeted Muscle Reinnervation (TMR), in which residual arm nerves are transferred to residual chest or upper-arm muscles (Kuiken et. al. 2009). Due to the limb loss, muscles are denervated and are no longer biomechanically functional. Once the nerve is reinnervated to the pectoral muscles, these muscles serve as the biological amplifier of motor commands, thus, physiologically appropriate EMG signals is recorded in order to control robotic hands (Kuiken et. al. 2009). TMR has shown to control opening and closing of hand as well as extension and flexion of the elbow (Kuiken et. al. 2009). It has been shown that reinnervated sensory nerves, regenerated through the muscle out to the denervated skin overlying the transfer sites, are capable to provide sensory feedback (Marasco et. al. 2009).

The TMR technique is more suitable for higher level amputation such as transhumeral and shoulder-disarticulation amputations (Kuiken et. al. 2009, Micera et. al. 2012). Surgical failure, neuroma formation and limb pain are certain risk involved with TMR. Even though, TMR technique can possibly provide sensory feedback to amputee and contribute towards the development of closed loop system, patients currently rely on the visual and tactile feedback (Kuiken et. al. 2009, Kim et. al. 2012). It fails to provide proprioceptive information (Kuiken et. al. 2009, Marasco et. al. 2009) It is limited in providing 5-6 degree of freedom which cannot control the recently developed DEKA arm that has 18 degree of freedom (Miller et. al. 2008).

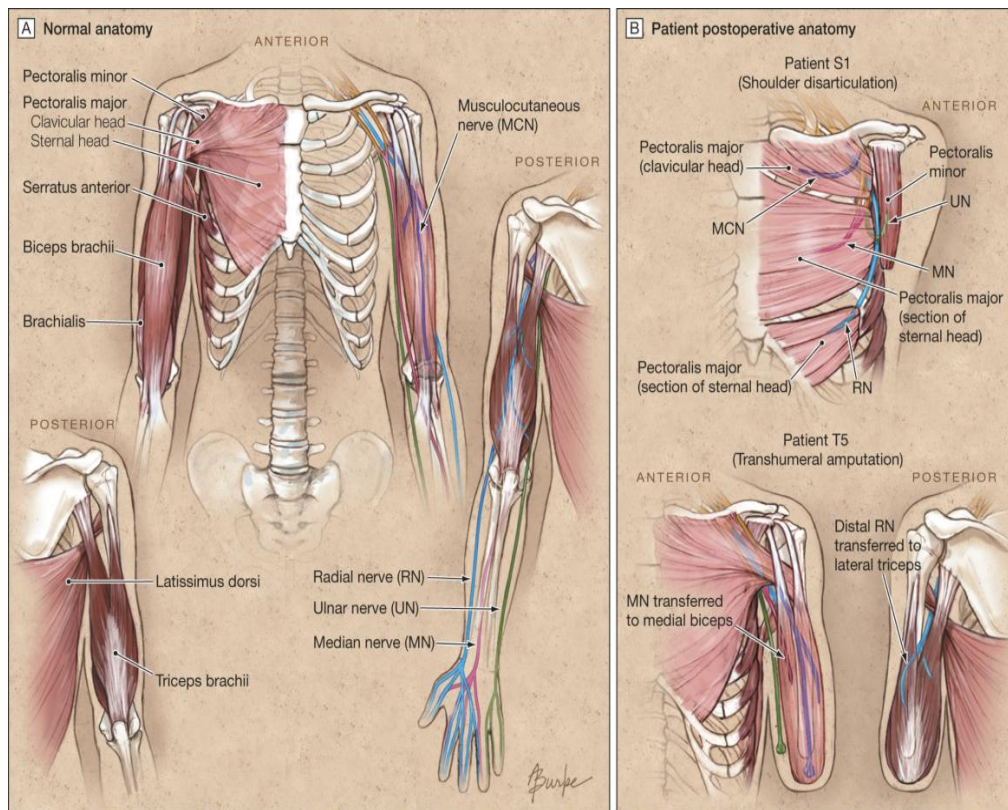


Figure 1.4 A) Normal muscular anatomy and innervations of the major muscles of the chest, shoulder, back, and arm. B) Examples of TMR surgery for patients with shoulder-disarticulation and transhumeral amputation in which the nerves innervating target muscles are cut, and nerves from the amputated arm are transferred to these muscles. Examples in T5 patient, the distal radial nerve was transferred to the lateral triceps muscle, leaving the long head of the triceps to provide EMG signals for elbow extension whereas the median nerve was transferred to the medial biceps to provide EMG signals for elbow flexion. (Kuiken et. al. 2009)

1.3.4 Cortical Interface

One of the aims of brain machine interfaces (BMI) is to obtain command signal from the motor cortex to control robotics prosthetics. One type of noninvasive BMI relies on Electroencephalography (EEG) electrodes recording of electric signals from the scalp, 2-3 cm away from the cortical surface, thus, reflecting the compound activity of many neurons (Donoghue et. al. 2002). Therefore it is low frequency content and less sensitive. The number of controllable degree of freedom using EEG BMIs is limited and relies on learning of non-natural control strategies that is not user intentional (Micera et. al. 2012).

The neural signal quality is improved with invasive recording if electrode is placed on the dura or cortical surfaces (Donoghue et. al. 2002). Recently, multi-electrode arrays (MEAs) have been designed to obtain intracortical recording of the action potential from individual neurons (Donoghue et. al. 2002). It has been shown to provide 3-4 degree of freedom controlling robotic prosthetics in both human and primates (Simeral et. al. 2011). Spike activity recorded from MEAs, implanted in motor cortex of monkeys, has been successfully decoded to provide real-time closed-loop neural control of cursor movement, and of robotic devices in two-dimensional space (Suner et. al. 2005). Recently, two tetraplegic subjects were implanted with 96-channel microelectrode arrays, and both were able to perform three-dimensional reach and grasp movements of robotic arm (Hochberg et. al. 2012). One of the participants was implanted with a multi-electrode array 5 years earlier, also used a robotic arm to drink coffee from a bottle as shown in Fig. 1.5 (Hochberg et. al. 2012). However, robotic reach and grasp actions were much slower with limited dimensionality as compared with able-bodied people (Donoghue et. al. 2002, Lebedev et. al. 2011, Hochberg et. al. 2012). Some of the current limitations of cortical BMI include the need of sophisticated signal processing that demand computationally intensive algorithms in order to decode neural activity and translated them into command signals (Lebedev et. al. 2006, Hochberg et. al. 2006). In addition, to fulfill the clinical intention multi-electrodes should be stable for years and record near to the neural bodies long-term. In

addition, in order to convey sensory perception to BNI users, microsimulation is required and since it is done in the cortex, and not in the nerve, its interpretation requires extensive learning (Donoghue et. al. 2002). Other issues that require improving of BMI technology include improving the quality of neural signals, development of better decoding algorithms, and obtaining long term performance (Lebedev et. al. 2011). Also, intracortical implantation of MEAs requires craniotomy surgery which is one of the ethical controversial topics.

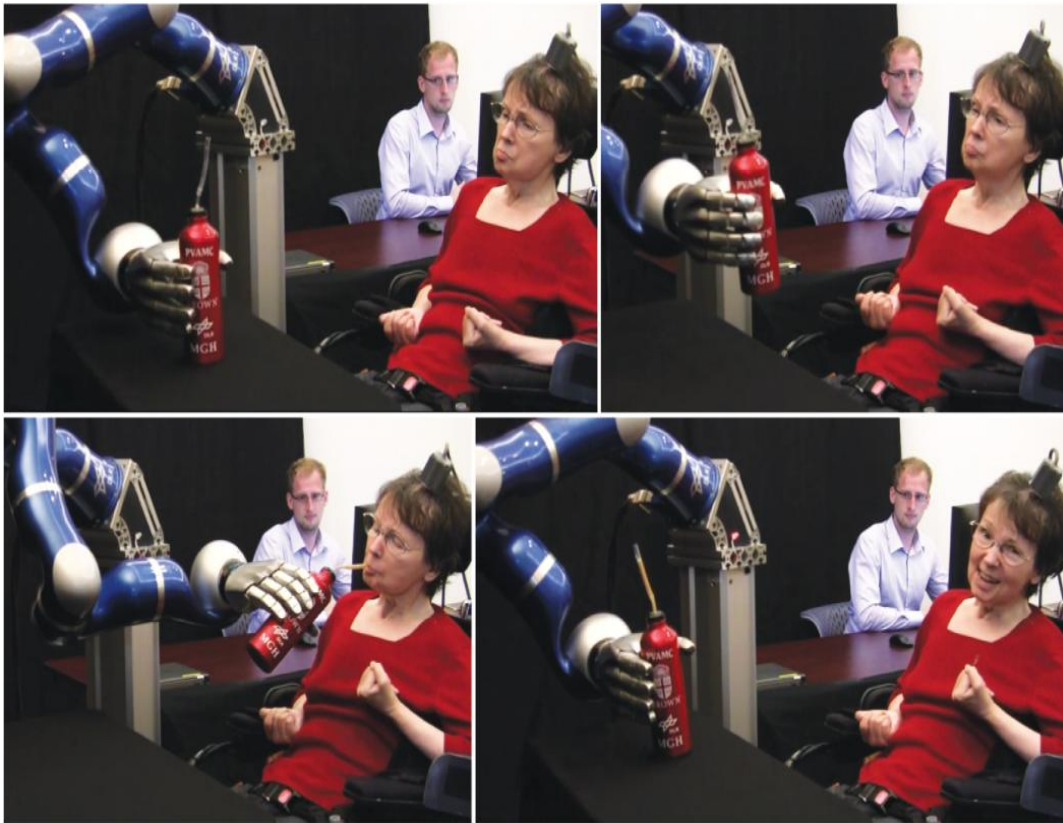


Figure 1.5 Tetraplegic 58-year-old subject using a BMI implanted in her motor cortex to control a robotic arm and grasp a water bottle. Her microelectrode was implanted 5.3 years before the beginning of this study. Across the five days, spiking signals were obtained from 41 of 96 electrodes (Hochberg et. al. 2012)

Table 1.1 Comparison between different Human–Machine Interfaces for the control of hand prostheses in amputees (Micera et. al. 2012)

Approach	Advantage	Disadvantage
Surface EMG	Non-invasive	Non- natural control strategies must be learnt by the subject
Implantable EMG	Improved quality over surface EMG signals	Non- natural control strategies must be learnt by the subject
Targeted Reinnervation	More natural control strategies, effective sensory feedback	Requires a surgical implantation but works with non-invasive signals. More suitable for amputation at shoulder level
Implantable Cortical Interfaces	Direct connection with the cortex	Too invasive
Non-invasive cortical interface	Non-invasive approach	Limitation in number of controllable degree of freedom. Non-natural control strategies.
Implantable peripheral Interface	Potentially effective and less invasive	Limitation in number of controllable degree of freedom and sensory feedback not clear

1.3.5 Peripheral nerve Interface

Peripheral Nerve Interface (PNI) is advantageous to cortical interface since electrode placement in peripheral nerve offer an easily accessible bidirectional flow of information from robotic arms to cortex and vice versa (Kim and Romero, 2012). Motor commands from the motor cortex are integrated and coordinated in the ventral motor neurons in spinal cord and can be recorded from motor axons in the peripheral nervous system. Conversely, sensory signals are directly elicited from the peripheral nerves by electrical stimulation which evokes the activity of the sensory cell bodies located in the dorsal root ganglia (DRGs). Such signals in the DRGs are sent to the thalamus and finally to the sensory cortex for limb awareness and movement coordination. While BMIs primarily records from cell bodies and dendrites of cerebral cortex, PNI record from axons, and evoking sensation through a PNI is naturally modulated by the spinal cord prior to reaching the somatosensory cortex (Kim and Romero, 2012). Therefore, better accuracy in the limb awareness and movement might be possible with the use of PNIs.

A number of PNIs have been developed and are currently classified according to selectivity, invasiveness, electrode design, and insertion mode (Fig. 1.6).

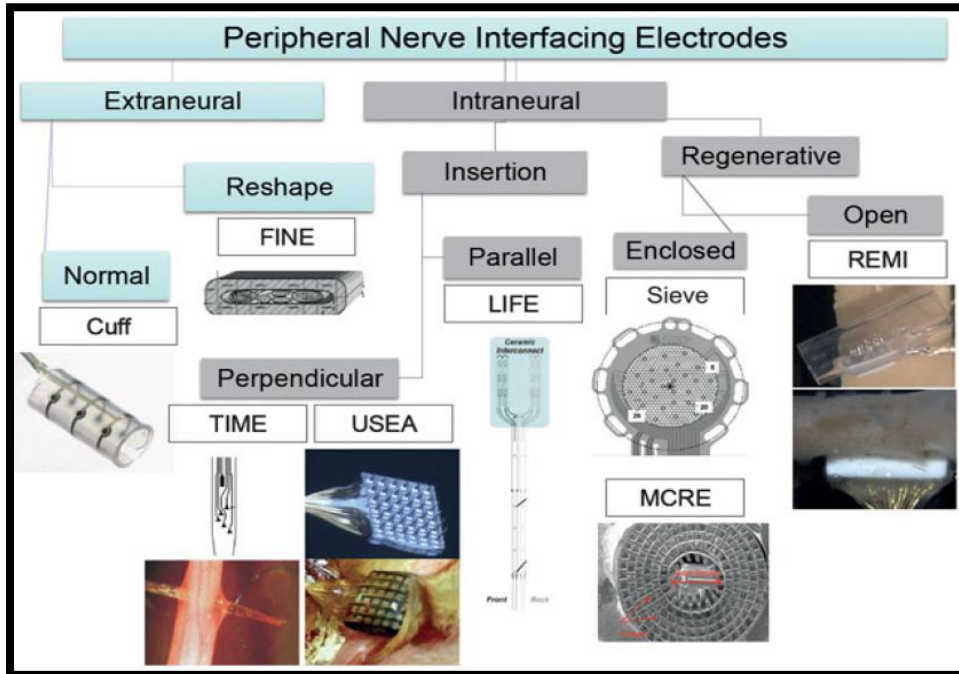


Figure 1.6 Classification of peripheral nerve interface electrodes. Extraneural electrode either normal cuff or reshaped FINE with minimum invasiveness, whereas intraneural electrodes are either insertion or regenerative. Regenerative interfaces include the sieve, micro-channel regenerative electrode and REMI designs (Kim and Romero, 2012)

1.3.5.1 Extraneural electrode

Extraneural electrodes such as cuff electrodes (Fig 1.7A) are embedded on an insulating tubular substrate and placed over the nerves. Spiral cuff electrode has been recorded 63 weeks after implantation, indicating a stable interface with the peripheral nervous system (Fisher, et. al. 2009). Some of the limitation of the cuff electrode is the results mechanical distortion and avoids the stimulating of neighboring nerve and tissue (Navarro et. al. 2005). Cuff electrodes are less likely damage the nerve and are easier to implant in comparison to penetrating or regenerative electrode (Fisher et.al.2009). However, the recorded activity of nerve is mutiunitary and the identification of signal spikes is not possible as the activity it records is a weighted average from entire nerve rather than from single axons (Navarro et. al.

2005). To avoid some of the initial limitations observed with the cuff electrodes, flat-interface nerve electrode (FINE) (Fig 1.7B) were developed by Durand and co-workers that are designed to reshape peripheral nerves into a favorable geometry for selective stimulation. Reshaping the shape of the nerve increases surface area of the nerve allowing more contacts to the electrode nerve interface. The FLAT has been demonstrated to have increased selectivity however, reshaping of the nerve by this electrode can cause nerve damage (Fig. 1.7B. Tyler et. al. 2002).

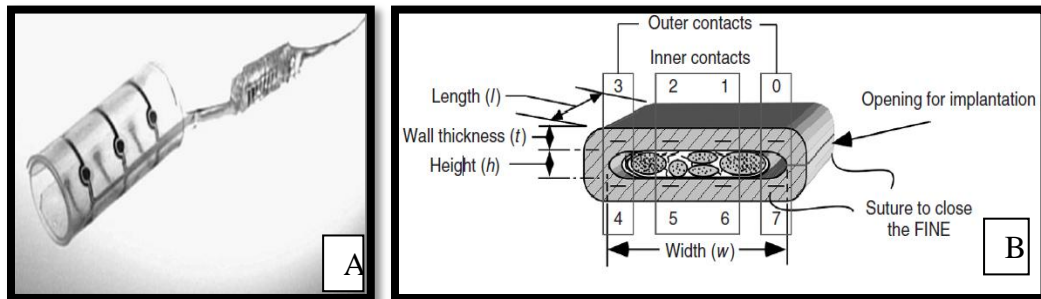


Figure 1.7 Extraneural electrodes A) silicone and hybrid silicone-polyimide cuff electrode. B) FINE electrode. (Navarro et. al. 2005; Tyler et. al. 2002).

1.3.5.2 Intraneural electrodes

Intraneural electrodes are placed directly into the peripheral nerve to record command signals for motor control and stimulate specific sensory modality axons (Navarro et. al. 2005). Intraneural electrodes are either insertion electrode (inserted parallel or perpendicular to the axons) or regenerative electrode (record from the regenerative axons). Moreover insertion electrodes are further classified according to the placement of the electrode in the nerve such as intrafascicular or intraneuronal (penetrating).

Various types of intrafascicular electrodes have been designed such as longitudinally implanted intrafascicular electrodes (LIFE), transverse intrafascicular electrodes (TIME) and coiled wire intrafascicular electrodes (CWIE) (Lefurge et. al. 1991, Boretius et. al. 2010, Bowman et. al. 1985). The LIFEs are constructed from thin insulated conducting wires such as Pt-Ir or metalized Kevlar fibers (McNaughton et. al. 1996, Lawrence et. al. 2003). The use of multistrand Kevlar LIFEs (m-polyLIFE) (Fig 1.8A) increases the tensile strength and signal-to-

noise ratio (Lawrence et. al. 2003) Moreover, poly-LIFE has been used short term to stimulate severed nerve proximal to the stump with upper limb amputee, and has elicited graded sensations of touch, joint movement and positions (Dhillon et. al. 2004). However, it is difficult to implant few of these electrodes into the different fascicles in order to selectively stimulate fiber bundles to the appropriate muscle groups (Navarro et. al 2005)

Further development in precision mechanics and micromachining technique have been introduced for multiunit electrode that carry a variable number of electrode sites mounted on the needle or incorporated into the glass, silicon or polyimide in 1D, 2D or 3D array (Navarro et. al 2005). Normann and his colleagues developed multi-electrode array (MEAs) known as the Utah slanted electrode array (USEAs) (Fig 1.8C), which consists of 100 needle electrodes (Aoyagi et. al. 2003). USEAs are inserted perpendicularly into the peripheral nerve using pneumatic insertion device (Aoyagi et. al. 2003). It has varying length of electrodes to provide access to most fascicles and to minimize the number of redundant electrode (Branner et. al. 2004). However, at the end of 7-month study, only 1 of 7 animals implanted with 100-microelectrode USEA in the sciatic nerve reported to be recording (Branner et. al. 2004). MEAs are capable of selectively recording from dorsal root ganglia (DRG) and has reported that in 76% of the 69 electrodes tested, the stimulus threshold was less than or equal to 3 μ A, with the lowest recorded threshold being 1.1 μ A (Gaunt et. al. 2009). However, DRGs contains sensory neurons, thus motor information cannot be recorded. It has been reported that MEAs (Fig 1.8B) are associated with poor tissue–electrode interface, tissue damage by probe micromotion within the soft nerve tissue, and electrode insulation due to tissue scar formation (Brain et. al 2005, Williams et. al. 2007).

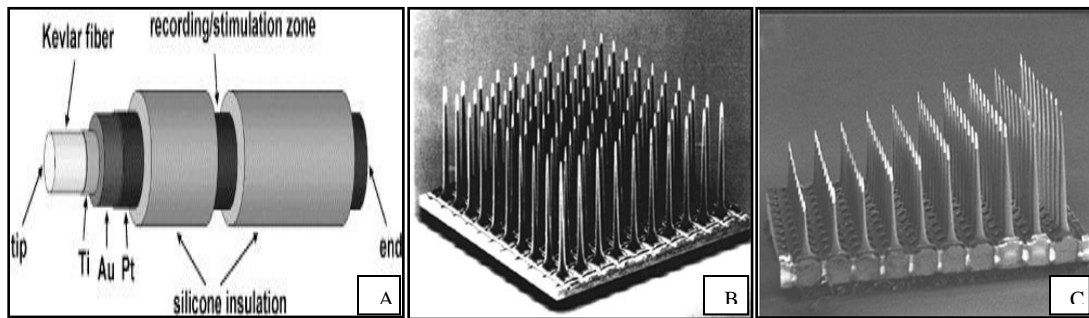


Figure 1.8 Examples A) polymer-based intrafascicular electrode (polyLIFE). B) Multielectrode array from University of Utah. C) Utah slanted electrode array. (Navarro et. al. 2005; Lawrence et. al. 2003; Aoyagi et. al. 2003; Branner et. al. 2004).

1.3.5.3 Regenerative electrode

Regenerative electrodes are designed to interface regenerated axons from a transected nerve, and their effectiveness depends on the biocompatibility, success of axonal regeneration, secondary nerve damage and adequacy of interface electronics (Lago, et. al. 2007). The severed nerves in the limb stump, that serve no specific function in amputees, are re-transected and allowed to grow through the electrodes, after which one can stimulate and record from the individuals regenerated axons (Kim and Romero 2012, lago et.al. 2007). Regenerative electrodes are considered to be more sensitive and invasive than insertion or penetrating electrode as it records from the individual regenerative axons. Three different types of regenerative electrodes have been developed, sieve regenerative electrode, multi-channel roll electrodes, and regenerative multi electrode array (REMI).

Sieve electrodes (Fig 1.9A) consist of the ring-shaped metal electrodes, which are placed around the sieve holes, through which the regenerative peripheral nerve fibers are directed (Ramachandran et. al. 2006). It records and stimulates the regenerating axons, when it grows through the sieve holes from the proximal nerve stump (Lago et. al. 2007). However, sieve electrode constricts the nerve fibers as they continue to grow thicker within the confine rigid electrode channel (Lago et. al. 2007). It eventually serves as a physical barrier and limits elongation of regenerating axons (Lago et. al. 2007).

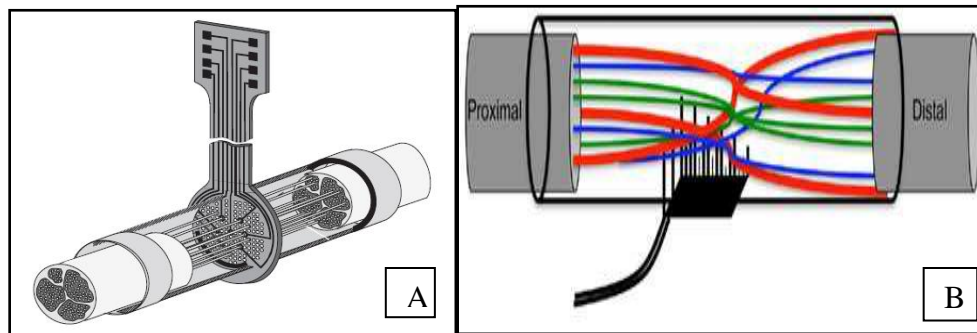


Figure 1.9 Regenerative electrodes: A) Sieve Electrodes, B) Regenerative Multi Electrode Array. Sources: (Navarro et. al. 2005; Lotfi et. al. 2011).

The REMI (Fig 1.9B) allows peripheral nerve regeneration through a non-obstructive multi-electrode array. It records single and multiunit activity in both acute and chronically damaged peripheral nerves (Garde et. al. 2009). This was demonstrated by the ability to record 300–1000 μV action potentials as early as 8 days post-implantation which was larger and more readily available compared to those reported using sieve electrodes, 100–200 μV with early recordings obtained at 29 days post implantation (Garde et. al. 2009). REMI consists of floating multi-electrode array (FMA) placed in the lumen of polyurethane tube that serves as the cuff for the regenerative axons (Garde et. al. 2009). The proximal and distal end of the transected nerve is sutured at each end of polyurethane tube respectively in such a way that regenerating axons grow through lumen crossing the electrode. REMI has shown to record as early as 8 days and as long as 120 days post implantation with high signal-to-noise ratio and minimal inflammation at the electrode implantation site (Seifert et. al. 2012, Garde et. al. 2009). It is also capable of selective stimulation or sensory feedback via segregation of neuron types using neuron-specific growth factors (Lotfi et. al. 2011). During the first few weeks of transected peripheral nerves undergo significant remodeling dependent upon the environmental milieu as discussed below.

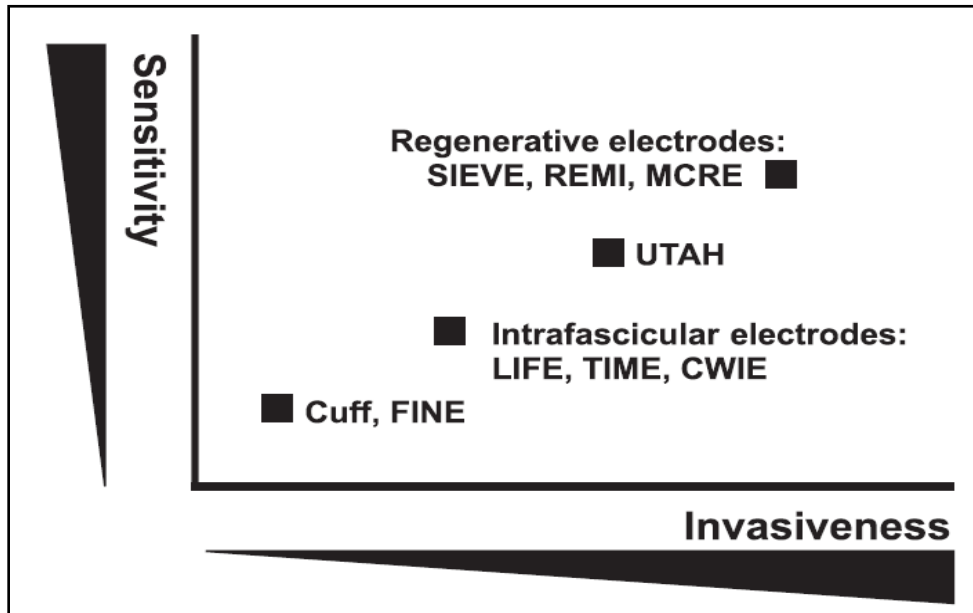


Figure 1.10 Classification of different types of peripheral nerve interface electrodes according to sensitivity and invasiveness. Extraneural electrode either normal cuff or reshaped FINE are less invasive and less sensitive compare to regenerative electrode (Kim et. al. 2012).

CHAPTER 2
PERIPHERAL NERVE REGENERATION

2.1 Introduction

Unlike the central nervous system (CNS), peripheral nervous system (PNS) is capable of spontaneous regeneration. Distinct cellular and molecular events have been defined as critical for successful regeneration in the PNS (Ide 1996, Kiryu-Seo et.al. 2011). Injured neurons activate a re-growing program which is mediated also by the interaction between the injured neurons and neighboring glial cells, and facilitated by a number of substrate adhesion molecules and their receptors as well as by several tropic factors (Allodi et.al. 2012). Various major events that occur after injury includes Wallerian degeneration, propagation of injury signal to soma, execution of regeneration program, axonal re-growth and target reinnervation. Various signaling pathways have to co-ordinate with neuronal and non-neuronal cell to achieve successful functional recovery which will be discussed below.

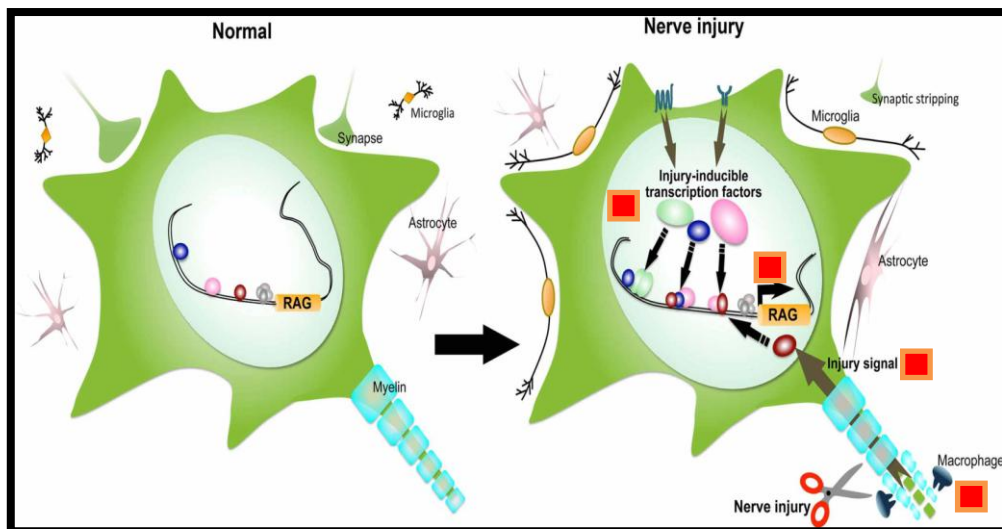


Figure 2.1 Major events that occurred after injury: a) Wallerian degeneration: degeneration of distal stump; infiltration of macrophage, phagocyte of myelin debris and damaged axons. b) Propagation of injury signal to cell body. c) Activation of transcription factors via cascade of

signaling pathways. d) Expression of regeneration associate genes (RAGs) (Kiryu-Seo et.al. 2011).

2.2 Neuronal changes occur at the injury site

The axons of both the myelinated and unmyelinated fibers are covered by the Schwann cells and enclosed by the basal lamina. The myelinated fibers form the Node of Ranvier, which is the internodal space between the myelin sheaths formed by Schwann cells (Ide 1996). After the axotomy of the nerve, distal stump is disconnected from the cell body which undergoes the degeneration process called Wallerian degeneration (Waller et.al 1850). The first signal of degeneration is observed within 24h after nerve injury, and prolonged for about 1–2 weeks (Navarro et.al. 2007). It is the myelin clearing process that prepares nerve to regenerate. Within 48 hours of injury, Schwann cells distal to the injury stop producing myelin proteins and then both myelinating and ensheathing Schwann cells divide, reaching peak proliferation around 4 days post-injury (Gaudet et.al. 2011, Trapp et. al. 1988, Stoll et.al. 1989). Macrophages infiltrate 2-3 days after injury at injury site due to the attraction by cytokines, such as monocyte chemoattractant protein 1, leukemia inhibitory factor (LIF) and interleukin (IL)-1 secreted by reactive Schwann cells (Navarro et.al. 2007, Tofaris et.al. 2002). Macrophages are activated along with Schwann cell and undergo the process of phagocytosis within a week (Gaudet et.al. 2011, Stoll et. al. 1999). Myelin debris and damaged axons are completely removed within two weeks from the distal stump via phagocytosis (Stoll et. al. 1999, Brück et.al. 1997). The growth of the uninjured PNS is suppressed by the inhibitory factors such as chondroitin sulfate proteoglycan of extracellular matrix and myelin associated inhibitors, which are removed during Wallerian degeneration (Zuo et.al. 2002, Mukhopadhyay et.al. 1994).

The proliferated Schwann cells coordinate with basement membrane to form the Bands of Büngner (Bunge et.al. 1982). These bands of Büngner are very important in guiding the growth cone, which are the re-growing axonal sprouts from the proximal stumps to the distal end. Growth cones are emerged from the severed axons and elongate along the guidance structure, bands of Büngner (Ide, 1996, Navarro et.al. 2007, Gaudet et.al. 2011). Otherwise, the

growth cones will make a tortuous course with the nearby connective tissue and form a neuroma (Navarro et.al. 2007, Fried et. al. 1991). These neuromas consist of large number of unmyelinated fibers in the chaotic orientation that is encapsulated in significant connective tissue stroma (Cravioto et. al. 1981).

The interaction between re-growing axons, Schwann cells and basal lamina is maintained by various adhesion molecules such as: cadherins, immunoglobulin cell adhesion molecules, and integrins (Allodi 2012, Huber et.al. 2003). Moreover, the orientation of the growth cone is facilitated by chemotactic events such as the gradient of neurotrophic and neurotropic factors (Mueller et. al 1999). Neurotrophic factors are diffusible molecules such as Nerve Growth Factor (NGF), Glial-cell Derived Neurotropic Factor (GDNF), Brained Derived Neurotropic Factor (BDNF) or Neurotrophin-3 (NT3). Other growth regeneration cues are substrate-bound such as laminin, fibronectin and collagen. Regenerated axons eventually reinnervated to their targets such as muscles or skin.

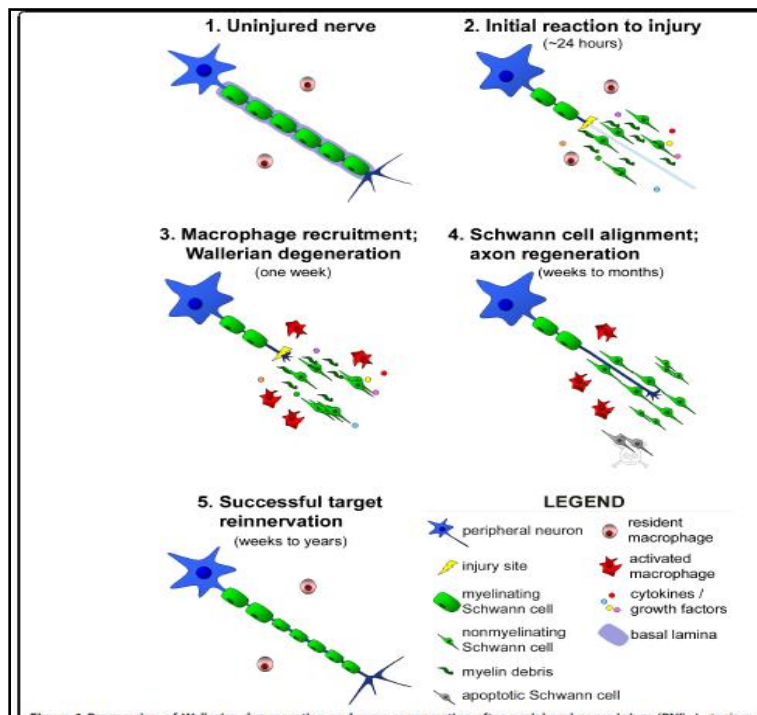


Figure 2.2 Regeneration process of Peripheral nervous system: Myelin sheath detached from Schwann cell distal to the injury. Cytokines are released and macrophages are activated. Myelin

debris and damaged axons are removed via phagocytosis. Alignment of Proliferated Schwann cells formed bands of Bungers where grown cone travels from proximal to distal end. (Gaudet et al. 2011)

2.3 Axonal Injury signal to soma

Neuronal regeneration requires the specialized signaling mechanism between injury site and soma in order to acquire the accurate and timely information about the nature and extent of axonal damage and also to execute an appropriate cell body response (Rishal et. al. 2010, Ben-Yaakov et.al. 2012). The injury signals required for survival and maintenance of regenerative neurons occur at sequential time phase. The excess entry of sodium and calcium ions leads to increase in action potential, followed by increase in calcium and cAMP levels (Allodi et. al. 2012, Patodia et.al. 2012, Navarro et.al. 2007, Rishal et. al. 2010, Patodia et. al. 2012). The abnormal burst increase in action potential at injury site is the first signal to warn the soma about the injury (Mandolesi et. al. 2004, Michaelevski et. al. 2010). The morphological changes that occur at neuronal cell body after receiving injury signals are chromatolysis, nuclear eccentricity, nuclear and nucleolar enlargement, and cell swelling (Fu et.al.1997, Navarro et.al. 2007). Chromatolysis means the dissolution of Nissl bodies which is associated with the anabolic response of cell body. The biochemical changes that occur in axotomized neurons include the reduction in DNA repression, increase in RNA and protein synthesis and decrease in the synthesis of neurotransmission-related products (Navarro et.al. 2007).

On the other hand, disconnection of normal supply of retrograde transported molecules such as trophic factor signals from innervated target and arrival of new signals from injury site serves as the negative signal (Michaelevski et. al. 2010, Patodia et. al. 2012). The cytoskeleton and associated motor proteins plays a critical role in axonal transport. The large numbers of retrogradely transported proteins such as STAT3, MAPK, ATF-3 have been identified in peripheral nerve following injury (Ben-Yaakov et. al. 2012, Michaelevski et. al. 2010). The microtubule dependent motor complexes, dyneins and kinesins serve as the mediators of retrograde and anterograde transport within the axons (Cosker et.al. 2008, Ben-Yaakov et. al.

2012). Dyneins mediates the retrograde transport of post-translation modification proteins from terminals towards the cell body (Rishal et. al. 2010, Cosker et.al. 2008, Ben-Yaakov et. al. 2012). The retrograde transport of de novo activated molecules to the cell body takes place within 12-24 hrs after injury (Patodia and et.al. 2012, Raivich et. al 1991, Patodia et. al. 2012). Ten-fold decrease in the level of retrograde transport of nerve growth factor (NGF) after sciatic nerve axotomy serves as the negative signal to soma (Raivich et. al. 1991), as continuous supply of NGF delays regeneration (Gold 1997). Several studies suggest that transcriptional factor such as ATF3, STAT3, CREB are locally synthesis in axons and retrogradely transport to cell body (Ben-Yaakov et. al. 2012). Thus the trophic molecules released from the injured environment, retrograde transport of activated molecules and all those positive and negative signals in turn activates the cascades of signaling pathway such as mitogen-activated protein kinases (MAPK), extracellular signal-regulated kinase [ERK], p38, c-Jun N-terminal kinase [JNK]), Janus kinases (JAK)/signal transducers and activators of transcription (STAT), Ras/Raf, phosphatidylinositol 3 kinase (PI3K)/AKT, abl, mammalian target of rapamycin (mTOR) and Mstb3 pathways (Allodi and et. al. 2012, Patodia et.al. 2012, Navarro et.al. 2007, Patodia et. al. 2012). These activated pathways in turn activate different transcriptional factors, which are involved in the expression of specific genes required for survival and regeneration process (Allodi and et. al. 2012, Patodia et.al. 2012, Navarro et.al. 2007, Ben-Yaakov et. al. 2012).

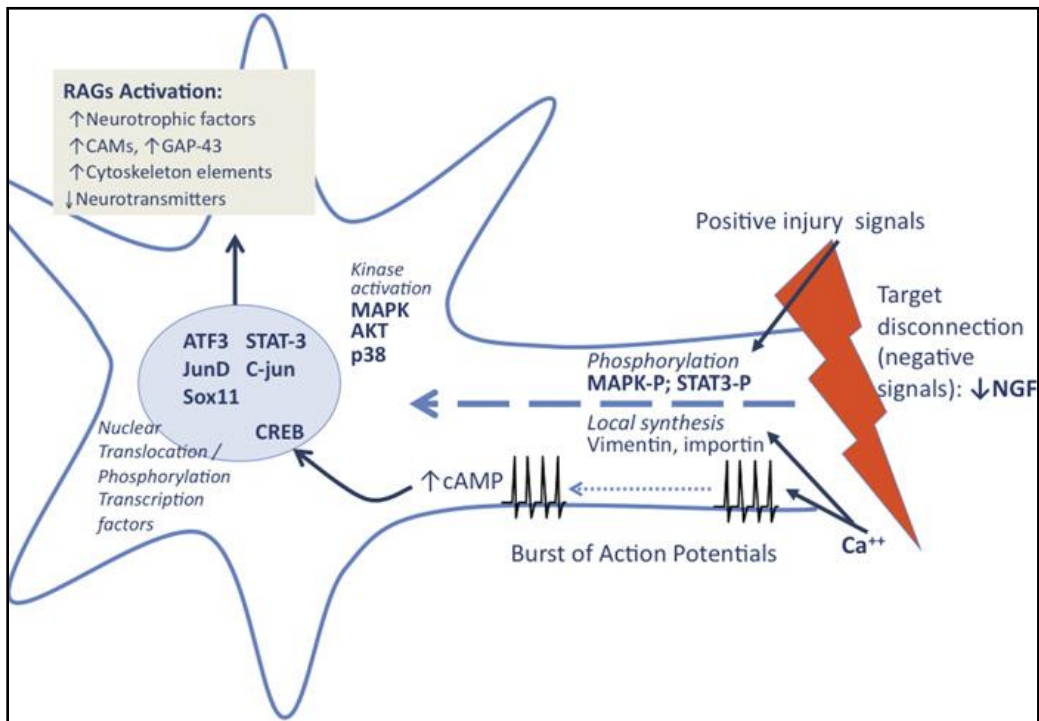


Figure 2.3 Injury signals to cell body include: abnormal increase of action potentials, increases cAMP level; disconnection of retrograde axonal transport of NGF; retrograde transport of locally synthesis transcriptional factors such as STAT3 and activation of cascades of signaling pathways. Nuclear translocation and phosphorylation of transcriptional factors activates several RAGs. (Allodi et.al. 2012)

2.4 Gene regulation and Transcriptional factors

After axotomy, neurons switch from transmission state to a growth state with changes in the expression of genes that encode for transcription factors. These factors in turn regulate the expression of genes involved in cell survival and neurite outgrowth (Allodi and et. al. 2012). Retrograde transport of axonal injury signals activates several signaling pathways genes at cell body that are responsible for either cell death or regeneration (Navarro et.al. 2007). In response to the environment cue following injury, transcriptional factors and their network regulate the gene expression according to the regeneration program (Kiryu-Seo et.al. 2011). Transcriptional factors are the proteins that bind to the specific DNA sequence activating or repressing the recruitment of RNA polymerase to transcribe the genetic information form DNA to RNA. Within 1-4 days after injury, neuronal cell body activates the vast number of regeneration associated

genes (RAGs) (Patodia et.al. 2012). RAGs are involved in cell-cell signaling, axonal growth and sprouting and also involved in the activation of the non-neuronal cellular milieu (Patodia et.al. 2012, Patodia et. al. 2012). Activation of intrinsic growth capacity produces neurotrophic factors such as NGF, brain-derived neurotrophic factor (BDNF), glial cell line-derived factor (GDNF), and neurotrophin-3 (NT-3); cytokines such as leukemia inhibitory factor (LIF), ciliary neurotrophic factor (CNTF), interleukin-6 (IL-6), and chemokines; chemoattractants like chemokine; neuropeptides like calcitonin gene-related peptide (CGRP), galanin, and vasoactive intestinal peptide (VIP); cell adhesion molecules like CD44, integrin, and L1 and numerous extra- cellular matrix (ECM) molecule (Kiryu-Seo et.al. 2011).

Transcriptional factors serve as the mediator between the injury signals and downstream proteins expression via regulation of RAGs (Patodia et.al. 2012). Data from phospho-proteomic and microarray studies have identified 400 signaling networks connected to 39 transcriptional factors in sensory neurons response after axonal injury (Michaelevski et. al. 2010, Patodia et. al. 2012). Injury-mediated transcriptional factors include c-Jun, JunD, activating transcription factor3 (ATF3), cAMP response element binding protein (CREB), signal transducer and activator of transcription (STAT3), CCAAT/enhancer binding proteins (C/EBPs), p53, Oct-6, nuclear factor kappa-light-chain-enhancer of activated B cells (NF- κ B), nuclear factor of activated T-cells(NFATs), Kruppel-like factors (KLFs), c-Fox, Sox11, SnoN, ELK3, AKRD1, NFIL3, Smad1, P311, and E47 among others (Allodi and et. al. 2012, Patodia et.al. 2012, Navarro et.al. 2007, Kiryu-Seo et.al. 2011, Patodia et. al. 2012, Herdegen et. al. 1998). The interplay of these transcriptional factors and the mechanisms behind the gene regulation is complex and has not been well established. However, the role of c-Jun, ATF-3, STAT3 has been well defined in nerve regeneration.

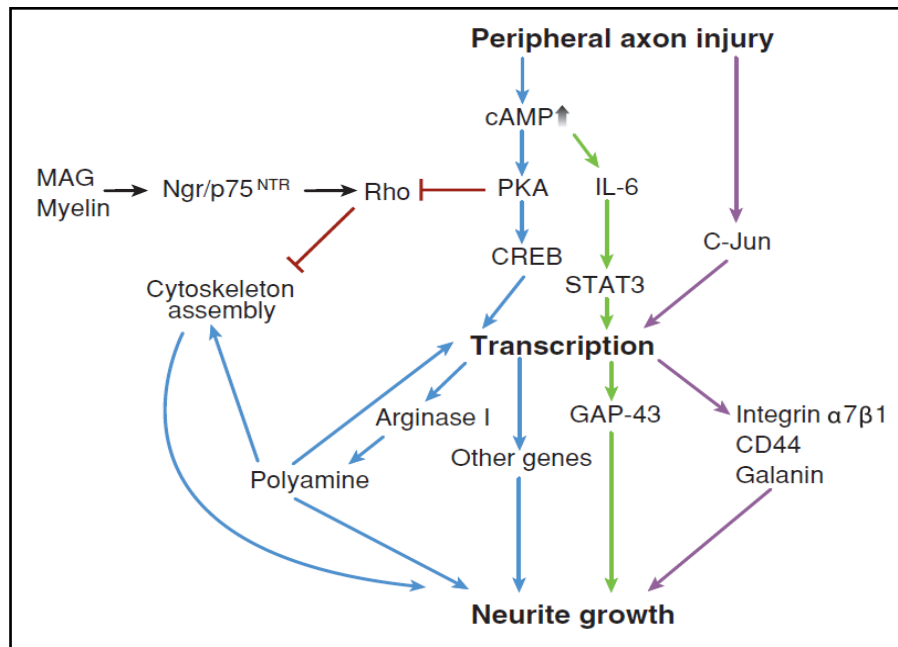


Figure 2.4 Various injury signals increase the level of cAMP, which in turn activate STAT-3 and CREB. In turn, c-Jun activates GAP-43 which increases neurite growth. (Chen et. al. 2007).

2.4.1 Activation Transcription factor-3 (ATF3)

ATF-3 is a stress inducible transcriptional factor that belongs to the ATF/CREB family. It forms homo and hetero dimmers with other basic leucine zipper domain transcriptional factor of the AP-1 family such as c-Jun, c-fox, and ATF-2. Normally, it is expressed a low level in the neuronal cell body, and its expression and nuclear translocation is stimulated after PNS injury but not in response to CNS injury (Saito et. al. 2008, Tsujino et. al. 2000, Seiffers et. al. 2006). Therefore, ATF-3 is considered as an early neuronal marker for nerve injury (Tsujino et. al. 2000). ATF-3 expression is activated by neurotrophin deprivation and JNK/SAPK and p53 dependent mechanisms (Patodia et. al. 2012, Saito et. al. 2008). It has also been reported that ATF-3 acts as the retrograde signal initiated after axonally transport from the injury site to the soma (Ben-Yaakov et. al. 2012).

Reduction of ATF-3 expression in neurons and Schwann cell correlates to axonal growth (Saito et. al. 2008). In addition to its role as an injury induced factor, ATF3 promotes neurite outgrowth, particularly in sensory DRG neurons (Seiffers et. al. 2006). It also prevents JNK mediated neuronal death and induces the expression of RAGs such as heat shock protein

27 (Hsp27), SPRR1A and c-Jun, which enhance the neurite outgrowth (Patodia et. al. 2012, Seijffers et. al. 2006, Nakagomi et. al. 2003). Even though ATF-3 contributes to nerve regeneration, up regulation of this factor is not sufficient to recapitulate the peripheral nerve regeneration program (Seijffers et. al. 2006). It has been reported that ATF-3 forms heterodimer with c-Jun to enhanced transcriptional activation of several RAGs (Patodia et. al. 2012, Kiryu-Seo et.al. 2011).

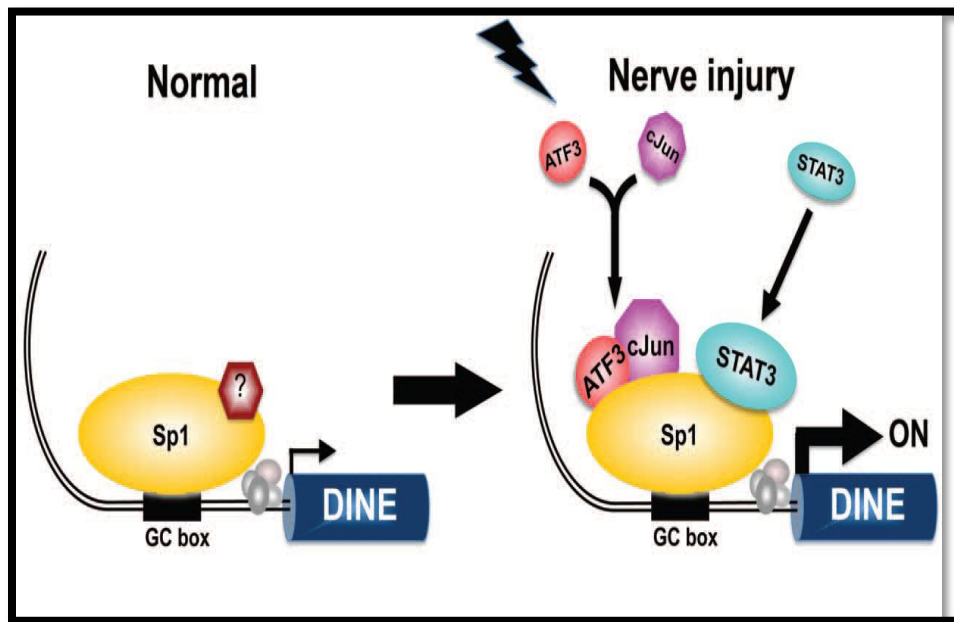


Figure 2.5 Transcriptional regulation of regeneration associate gene, Damage-induced neuronal endopeptidase (DINE): Before injury, Transcriptional complex express DINE at low level. Following injury, injury-inducible transcriptional factor ATF3 form a heterodimer with c-Jun and Sp1 provides a platform to recruit ATF3, c-Jun, and Stat3 which express DINE at higher level. (Kiryu-Seo et.al. 2011).

2.4.2 c-Jun

The activator protein-1 (AP-1) transcriptional complex is a well-characterized gene regulator pathway activated in response to various stimuli including cytokines, growth factors, injury and infections. It controls cellular process including differentiation, proliferation and apoptotic.

c-Jun is one of the primary component of the AP-1 complex where it forms homo dimer with Jun family and hetero dimer with c-fox and ATF/CREB family (Kiryu-Seo et.al.

2011, Herdegen et. al. 1998). It is produced after injury as an immediate early gene and remains at the high level in injured neurons throughout the regenerative process (Patodia et. al. 2012, Herdegen et. al. 1998). Schwann cell also upregulate c-Jun where it negatively regulate myelin formation but induce local inflammation (Kiryu-Seo et.al. 2011, Wilton et. al. 2009). Several studies of c-Jun via target gene deletions or pharmacological inhibition suggest the tripartite role of c-Jun in 1) neural degeneration, 2) inflammation and 3) repair (Patodia et. al. 2012). Deletions of c-Jun strongly reduce the speed of axonal regeneration and perineuronal sprouting; significantly delay functional recovery and also diminished microglia and astrocyte activation and T-cell influx (Kiryu-Seo et.al. 2011, Patodia et. al. 2012, Raivich et. al. 2004, Makwana et. al. 2010). Furthermore, c-Jun deletion reduced expression of RAGs including cell adhesion molecule such as integrin $\alpha 7\beta 1$ and CD44 and also neuropeptides such as galanin (Kiryu-Seo et.al. 2011). It also reduces successful target reinnervation 4-5 fold (Raivich et. al. 2004). The role of c-Jun in cell survival is illustrated by the report in which c-Jun mutants showed the survival of facial motor neurons after axotomy, but surviving neurons were severely shrunken (Herdegen et. al. 1997, Patodia et. al. 2012). Therefore, c-Jun has a significant role in switching on the regeneration program and regulates apoptosis.

Activation of c-Jun mediated transcription depends upon the chemical modification of three different sites: the N-terminal phosphorylation at serines 63 and 73 and threonines 91 and 93 residue, dephosphorylation of Thr239 and the acetylation of lysine residues in the basic, near C-terminal region aa257–276 (Patodia et. al. 2012, Raivich 2008). The chemical modification is directly or indirectly control by different component of MAPK family such as phosphorylation kinase JNK 1, 2 and 3; extracellular signal regulated kinase ERK 1 and 2; p38 MAPK isoforms (Raivich 2008). JNK is activated after injury and is retrogradely transported to the cell body along with upstream kinases, MEKK and JNK interacting proteins, JIP (Raivich 2008, Patodia et. al. 2012). Prolonged activation of JNKs in DRGs has been reported after sciatic nerve injury (Kenney et. al. 1998). Accumulation of N-terminal phosphorylation has

shown neuronal death (Kiryu-Seo et.al. 2011) whereas inhibition of JNKs reduces the expression of c-Jun and ATF-3 and decrease axonal growth (Lindwall et. al. 2004). The effect on regeneration is considerably smaller in JNK mutants than c-Jun deletion (Patodia et. al. 2012). Therefore, the regeneration effect of c-Jun dependent or independent to N-terminal phosphorylation is still controversial.

Table 2.1 Effects of Transcriptional factor c-Jun deletions and ATF-3 over expression on peripheral nerve regeneration

Gene	Modification	Effects	References
c-Jun	Neuronal c-Jun knockout	Strongly reduced target re-innervation Decreased RAG expression and neuronal sprouting Delayed functional recovery	Raivich et. al. 2004 Makwana et. al. 2010
ATF-3	ATF-overexpression	Enhanced speed of regeneration in mice constitutively expressing ATF3 in DRGs	Seijffers et. al. 2006

2.5 Current Limitations

Despite the advancement in neural prosthetic devices, current limitations of nerve interface persist with lack of proprioceptive feedback, invasiveness and lack of long-term reliability. Recently developed REMI with an open architecture for the nerve to regenerate, overcomes the limitation of sieve electrode by reducing the axonopathy. It has been reported previously that acutely injured or implanted after months of chronic amputation, could be interfaced early by enticing them to grow in close proximity to electrodes placed in a tridimensional open REMI (Seifert et. al. 2012, Garde et. al. 2009). Even though, the number and frequency of action potentials recorded by REMI was increased in first two week after implantation, reduction in the number of recording electrodes has been observed over time (Seifert et. al. 2012). The mechanisms that lead to failure in the REMI are unknown. Micromotion caused by limb stretching may be a possible cause of signal deterioration by the REMI, in which case a persistent expression in ATF-3 and c-Jun are expected. This study will

evaluate the expression levels of these two transcription factors in REMI implanted animals to determine if micromotion plays a significant role in signal decay.

2.6 Specific Aims of the project

This study evaluates if stability of REMI at nerve-interface is a cause of signal decay overtime in acute as well as in sub-chronic injury animal model. To specific aims has been purposed to study micro-motion at REMI/Nerve interface in acute as well as in sub-chronic injury as follows.

2.6.1 Specific Aim 1

To determine if nerve stretching at 70% (moderate Stretched) and 100% (excessive stretched) limb extension causes micro-motion, related tissue damage or interferes with regeneration in REMI implanted acute injury animals, by analysis of transcription factors in DRG cell bodies.

Sub aim 1: To evaluate the expression levels of ATF3, a neuronal injury marker, in moderate Stretched and excessive stretched animals and to compare with unstretched animals.

Sub aim 2: To evaluate the expression levels of c-Jun, a neuronal regenerative marker, in moderate stretched or excessive stretched animals and to compare with unstretched animals.

2.6.2 Specific Aim 2

To determine if REMI-implanted animals undergo micromotion, related tissue damage or have continued regeneration in sub-chronic injury animals, by analysis of transcription factors in DRG cell bodies.

Sub aim 1: To evaluate the expression levels of ATF3, a neuronal injury marker, in sub-chronic injury and to compare with acute injury.

Sub aim 2: To evaluate the expression levels of c-Jun, a neuronal regenerative marker, in sub-chronic injury and to compare with acute injury.

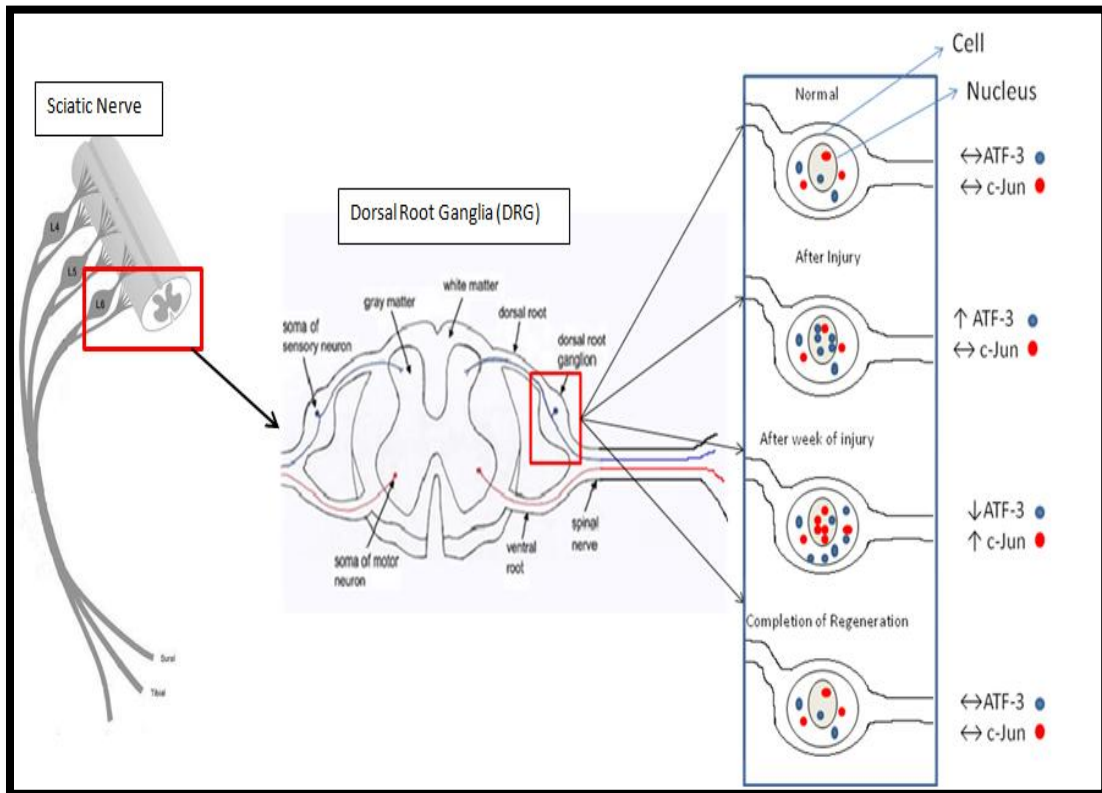


Figure 2.6 Diagram of the expected results in the expression of ATF-3 and c-Jun in normal and injured animals at different stages after recovery. It is expected that after injury ATF-3 and c-Jun will increase in expression and translocate to the nucleus, subsiding after regeneration at 30 and 60 days. If micromotion induced continues nerve injury, the levels of nuclear ATF-3 and c-Jun are expected to be increased over non-injured levels at all times.

CHAPTER 3

SPECIFIC AIM 1: TO STUDY WHETHER THE NERVE STRETCHING DUE TO LIMB EXTENSION AFFECTS NERVE GERENERATION AND MICROMOTION RELATED MICRO- INJURY AT REMI /PNS INTERFACE

3.1 Micro-motion

Implanted electrode size and electrode fixation procedure greatly influence tissue interaction in CNS (Thelin et. al. 2011). Electrode movement around the tissue called micro-motion could exacerbate local damage to the nerve. Tethering silicon microelectrode arrays to the skull increases the cortical brain tissue response in the recording zone, surrounding the microelectrode array, as compared to the untethered (Fig 3.1). Tethered electrode causes increase inflammatory response leaving an oval shaped cavity representing the brain movements within the skull (Fig 3.1(C)) whereas untethered electrode moves along with the brain tissue (Fig 3.1 (D)) resulting no effects of micromotion. Besides the initial inflammatory response to cortical electrode insertion, microscale movements of the tethered electrode arrays are considered to be important factors for continuous nerve injury (Thelin et. al. 2007). Chronic inflammation at the microelectrode brain tissue interface is considered to be an important factor for chronic recording failure (Biran et. al. 2005). Plastic needle-like device implanted into brain tissue elicits a greater foreign body response when anchored to the skull than when left floating in isolation, providing evidence that motion of an implanted hard object with respect to the surrounding tissue increases inflammation at the interface (Lee et. al 2005).

Electrode-tissue elasticity mismatches progressively exacerbate the chronic foreign body responses which eventually damage the nerve, including neural and dendritic loss (Kim and Romero 2012). The fabricating materials used for microelectrodes such as Silicon and

Platinum/Iridium has Young's modulus in the range of 135 GPa-165 GPa (Cheung 2010) whereas that of Brain tissue is ~3 kPa (Taylor et. al. 2004) and that of nerve tissue range between 66 kPa and 266 kPa (Pfister et al. 2004). Peripheral nerves are intrinsically elastic; electrode micro-motion may induce continued tissue micro injury leading to increase in distance between neurons and electrode. The function of the electrode will be compromised if the distance between electrode and neurons is increased either by loss of neurons in close vicinity to the electrode or by progressively growing glial capsule (Thelin et. al. 2007, Brain et. al. 2007). It has previously been reported that REMI neither causes micro-injury nor affects regeneration in an acute injury animal model (Khobragade et. al. 2011). However, animals are unable to move their limb after transection of the nerve, until the nerve is reinnervated to the muscles. It has not been studied if the nerve stretching due to limb extension causes micro-motion of the REMI-nerve interface and affects nerve regeneration. In this study, well established molecular marker as mention above in section 2.4; nerve injury marker ATF-3 and regenerative marker c-Jun, are used to evaluate tissue micro-injury and nerve regeneration at 30 days and 60 days after REMI implantation.

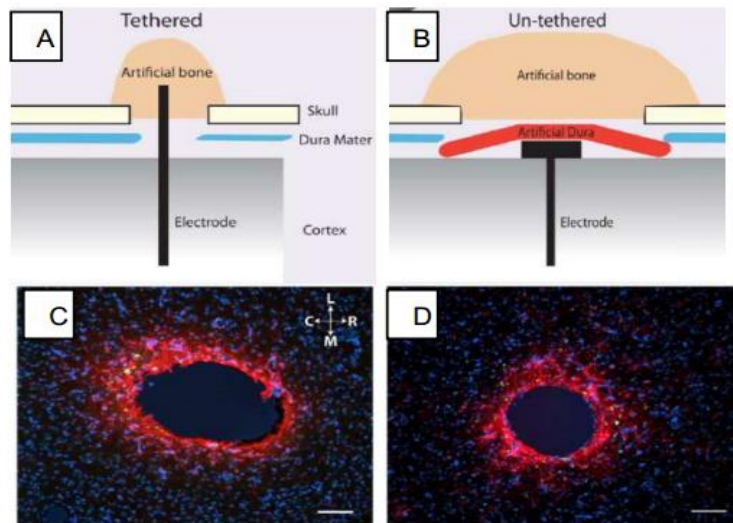


Figure 3.1 (A) Tethered mode of implantation, (B) Untethered mode of implantation, (C) & (D) Tissue reaction after 12 weeks of Implantation; immunohistochemically labeled for GFAP (red), ED1 (green) and DAPI (blue). (C) Cavity left by tethered electrode, (D) Inflammatory response around untethered electrode. (Thelin et al. 2011)

3.2 Materials and methods

REMI comprises of Floating Multi-electrode Array (FMA) placed in the polyurethane tube. FMA were custom made having the dimension of 2.45mm X 1.95 mm X 0.45 mm (Microprobes Inc. MD) and each FMA consists of 18 Platinum / Iridium (70 / 30 %) electrodes separated by 400 μ m and height range from 0.7 mm to 1 mm to maximize the neuronal contacts at different planes. The micro-electrodes are connected to the omnetics connector via Parylene-C insulated gold wires having 25 μ m diameter. The Omnetics connector is housed in the Titanium pedestal which serves as external interface for recording. The polyurethane nerve guide is filled with collagen I/III (0.3%; Chemicon, Temecula, CA, USA) and is sterilized a day prior to the surgery by Ultraviolet radiation.

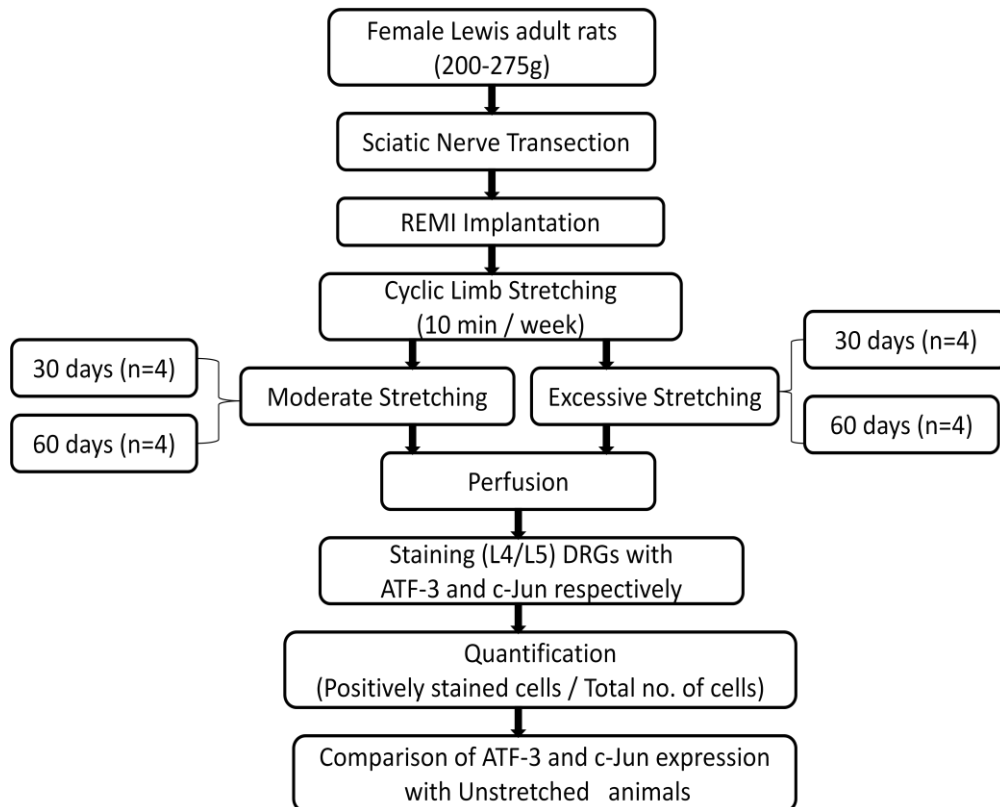


Figure 3.2 Experimental design of specific aim 1: After sciatic nerve transection, REMI was implanted followed by either 70% or 100% limb stretching. Limb stretching was not applied to control groups. After 30 days and 60 days time points, animals were perfused and L4-L5 DRGs were stained with c-Jun or AFT-3.

3.2.1 Surgery and Implantation

Nineteen female Lewis adult rats (200-275g) were used in this study (n=3 for uninjured as control and n=8 for REMI implant respectively for two time points: 30 days and 60 days; REMI implanted were further divided into n=4 for 70% stretching and 100% stretching for each points). The dorsal side of the pelvic and the left thigh regions were shaved after the animal reached at the adequate level of anesthesia indicate by the loss of corneal reflex, and the eyes were kept moist using an ophthalmic ointment. To provide from infection, 70% ethanol and povidone-iodine were applied to the surgical site.

The vertical incision was made through the skin in the pelvic region where tips of the exposed dorsal processes were removed and the pedestal was mounted on the pelvis after removing clearing the underlying muscle tissue and fascia. Bone cement (Biomet; Warsaw, Indiana, USA) was applied around the pedestal to hold it in place and the gold wires linked to the connector were passed subcutaneously to the biceps femoris muscle. Again the vertical incision was made on the left thigh where sciatic nerve was exposed and then transected after separating the femoris and the semitendinosus muscles were apart. The nerve endoneurium was sutured using 10-0, 140 µm mono-filament after inserting the proximal and distal stumps of nerve in the ends of sterilized REMI conduit respectively. The animals were applied with antibiotic ointment (Fougera, Triple antibiotic Ointment) on the surgical site. After regaining consciousness, the animals were injected with antibiotic (Cefazolin, 5 mg/kg) intramuscularly on the contralateral thigh and with pain control (Buprenorphine, 0.1 mg/kg) subcutaneously at the dorsal side of the neck. The procedure for 48 hours control animals were performed using collagen-filled tubes without the FMA and did not involve pedestal implantation. The surgical procedures were carried out in accordance with the guidelines of Institutional Animal Care and Use Committee (IACUC) of the University of Texas, Arlington.

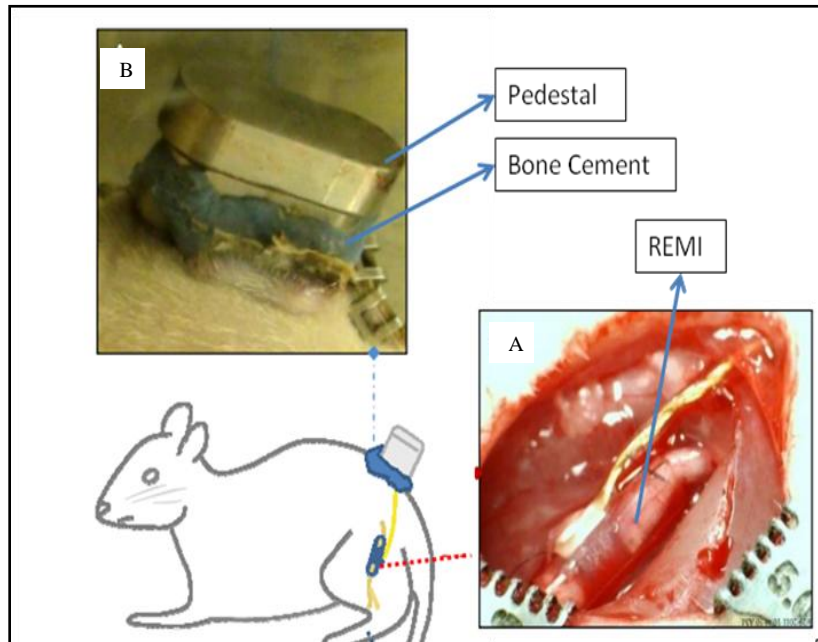


Figure 3.3 Surgery and Implantation: A) REMI implantation after the transection of sciatic nerve. B) REMI was covered with the pedestal for external interface and was hold by the bone cement (Khobragade 2011).

3.2.2 Stretching

Cyclic limb Stretching was applied to the left limb once a week. Position 1 is set in the actuator controls when the thigh is at 90° to the hip whereas position 2 is set when the leg is fully extended and is considered to be an excessive stretch, 100% stretch. Then the actuator is set to the cycle between position 1 and either 70% of the position 2 (moderate stretching) or 100% (excessive stretching) for 10 minutes at 20 mm/sec. Nerve strain due to limb extension was measured previously by Watson 2012, by measuring the change of length due to limb extension divided by the initial length. Previously reported, moderate limb stretching induces $18.3 \pm 1.0\%$ nerve strain while excessive limb stretching induces $34.7 \pm 1.3\%$ nerve strain (Watson 2012)

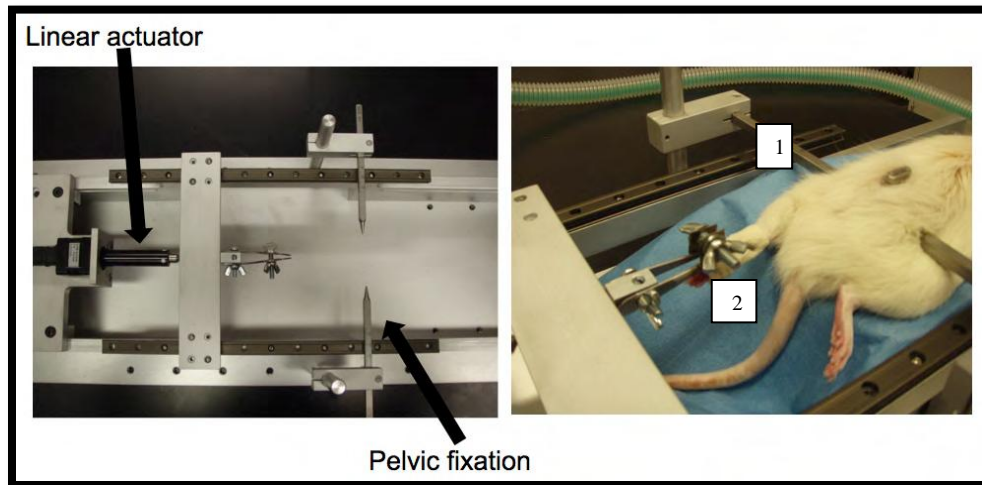


Figure 3.4 Limb stretching by using linear actuator and pelvic fixation device. Cyclic stretching either full length extension (100% stretching) position 1 or 70% of full length extension (70% stretching) position 2 was performed per weekly (Watson 2012)

3.2.3 Extracting Dorsal Root Ganglia (DRG)

The animals were euthanized via an intraperitoneal injection of sodium pentobarbital (100 mg/kg) after 30 days and 60 days post implantation. Then the animals were sacrificed by transcardial perfusion with 0.9% saline for 5 minutes followed by 4% Paraformaldehyde (PFA) for 15 minutes. The vertebral column were harvested and post-fixed overnight in 4% PFA and then transferred to 1X PBS (Phosphate Buffered Solution). Then the sciatic nerve was exposed which branches leading to L4 and L5 DRGs inside vertebral column. The ipsilateral and the contralateral L4 and L5 DRGs were extracted from the vertebral column by removing the bones above and around the DRGs. The harvested DRGs were kept in 1X PBS. The procedure was same for the 48 hours positive control animals but the perfusion was performed 48 hours after injury. Right DRGs were harvested using same procedure for uninjured control.

3.2.4 Sample preparation and Cryosectioning

The extracted DRGs were kept in 30% sucrose overnight for cryoprotection. DRGs were made embedded by freezing specimens in the Optimal Cutting Temperature (OCT) freezing media (Tissue Tek) using dry ice and 100% ethanol. The blocks were store in -80° C

which were sectioned at the thickness of 20 μm using Cryostat (Leica CM 1850) at -19°C to -21°C . The sections were mounted on positive-charged slides.

3.2.5 Immunofluorescence staining

The L4-L5 DRG sections were washed three times in 1X PBS for 10 minutes. To block non-specific binding, the slides were incubated for an hour with blocking solution. The sections were incubated overnight with primary antibody. The secondary antibody was added after washing three times in 1X PBS for 10 minutes and was incubated for 2 hours. DAPI was used as counterstained after secondary antibody. The sections were immune mount after washing the secondary antibody.

Table 3.1: Dilution factors of primary and secondary antibodies for cJun and ATF3 staining

Antigen	Blocking Solution	Primary Antibody/ Dilution	Secondary Antibody/ Dilution
cJun	4% Donkey Serum	Rabbit anti-cJun (Cell Signaling) / 1:300	DnaRb IgG Cy3 (Jackson Immunoresearch) / 1:300
ATF3	4% Donkey Serum	Rabbit anti-ATF3 (Santa-Cruz Biotechnology) / 1:100	DnaRb IgG Cy3 (Jackson Immunoresearch) / 1:300

3.2.6 Image Analysis and Quantification

Tissues were sectioned serially and one tissue section per animal was used for quantification of c-Jun and ATF-3 respectively. Slide selection was consistent with all the samples and was selected approximately consisting middle portion of the L4/L5 DRGs. Nuclei double staining with c-Jun and DAPI is considered as positively stained cells for c-Jun quantification and nuclei double staining with ATF-3 and DAPI is considered as positively stained cells for ATF-3 quantification. All the cell bodies in an entire section were counted. The percentage of cells expressing cJun or ATF-3 in L5/ L4 DRGs was calculated by dividing positively stained cells by total number of cells. The percentage of cJun and ATF-3 expression in 30 days and 60 days after injury with moderate stretching or excessive stretching were compared with uninjured animals respectively. The statistical analysis was performed using one way ANOVA followed by Newman-Keuls post hoc ANOVA test. The p-values less than or equal

to 0.05 were considered to be statistically significant. The results were reported as mean \pm standard deviation or mean \pm standard error of the mean. The number of stars indicates the significance level: one star (*) for p-value less than or equal to 0.05, two (**) for p-value less than or equal to 0.01 and three (***) for p-value less than or equal to 0.001.

3.3 Results

Unlike CNS, Peripheral Nerve System undergoes regeneration process following injury, due to its distinct morphology and cellular and molecular signaling pathways. Transcriptional factors play a vital role in activating the regeneration associate genes. Immediate early genes, ATF3 and c-Jun, are the essential components to initiate the process of nerve regeneration after sciatic nerve transaction as described in section 2.4. Injury marker, ATF3, protects the nerve and assists to activate the nerve regeneration program whereas regenerative marker, c-Jun, is required for axonal regeneration. The negative staining control of ATF-3 and c-Jun, without the primary antibody, is shown in the figure 3.5 whereas nucleus staining with DAPI and merge image with primary antibody is shown in figure 3.6. The positively stained c-Jun and ATF-3 ipsilateral L5 /L4 DRG of animals 48 hours after injury are shown in the figure 3.7 where higher level of ATF-3 and c-Jun expression was observed.

Atf-3 and c-Jun labeled ipsilateral L5 /L4 DRG of uninjured (control) is shown in figure 3.8. The representative image of ATF-3 expression in REMI implant with moderate limb stretching and excessive limb stretching at 30 days and 60 days after injury are shown in figure 3.9. The figure 3.10 shows the graph that compares the Atf-3 expression at 30 days and 60 days after injury with both moderate and excessive limb stretching. Quantitative analysis revealed that the percentage of ATF-3 expression decreased significantly from 30 days to 60 days with either moderate stretching ($12.76 \pm 2\%$ to $6.81 \pm 1.4\%$) or excessive stretching ($11.93 \pm 1.3\%$ to $1.68 \pm 1.3\%$). ATF-3 increased significantly at 30 days compared to uninjured animals ($4.9 \pm 0.31\%$) but was comparable at 60 days after injury. The representative image of c-Jun in REMI implant with moderate limb stretching and excessive limb stretching at 30 days

and 60 days after injury are shown in figure 3.11. The figure 3.12 shows the graph that compares the c-Jun expression at 30 days and 60 days after injury with both moderate and excessive limb stretching. The level of c-Jun expression decreased significantly with excessive limb stretching from 30 days ($49.69 \pm 16.77\%$) to 60 days ($3.31 \pm 2.2\%$) and that was comparable to the uninjured animals ($5.24 \pm 2.1\%$). No significant difference was observed in the c-Jun expression between excessive stretching ($49.69 \pm 16.77\%$) and moderate stretching ($42.71 \pm 7.2\%$) at 30 days. Also, no significant difference was observed with moderate stretching between 60 days ($40.14 \pm 20.38\%$) and 30 days ($42.71 \pm 7.2\%$)

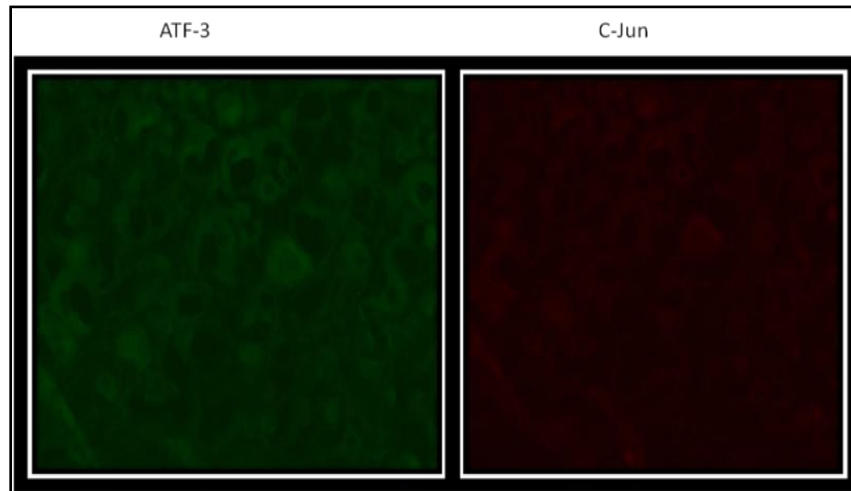


Figure 3.5 Negative Staining control: Ipsilateral L4/L5 DRGs with secondary antibody but without primary antibody of ATF-3 and c-Jun showing no specific staining of the secondary antibody.

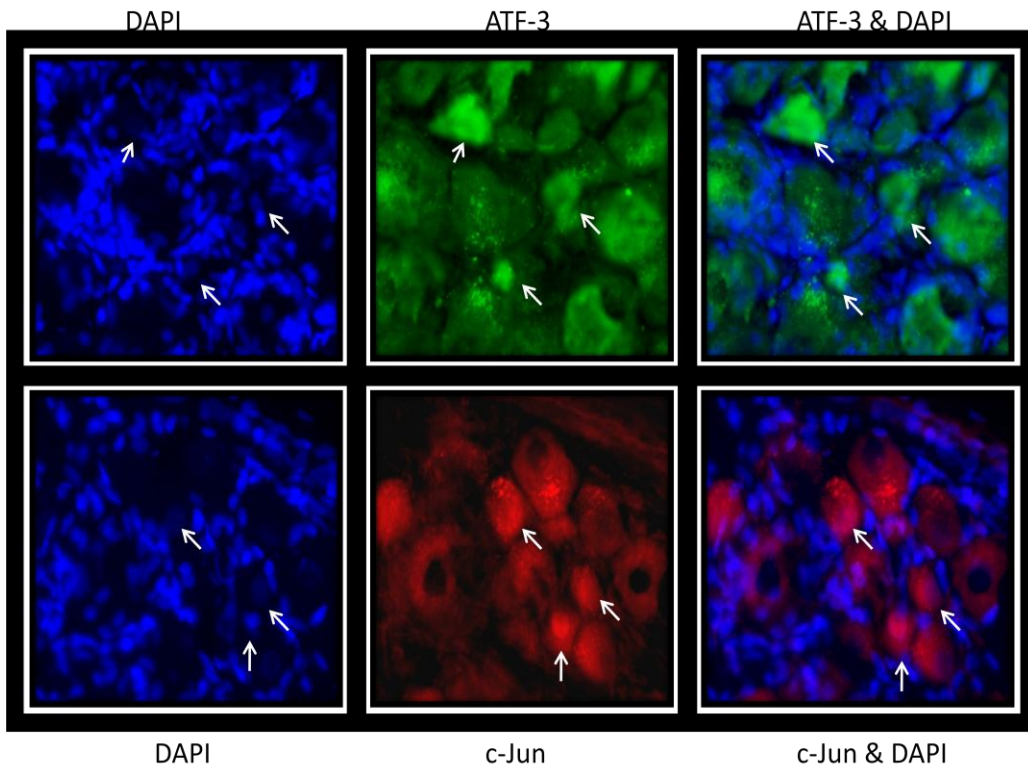


Figure 3.6 Counterstaining with DAPI as a nuclear marker. Ipsilateral L4/L5 DRGs Staining with ATF-3 and c-Jun with DAPI to validate the positive nucleus staining of ATF-3 and c-Jun. Green: ATF-3, RED: c-Jun, Blue: DAPI. Arrow indicates the positive cells.

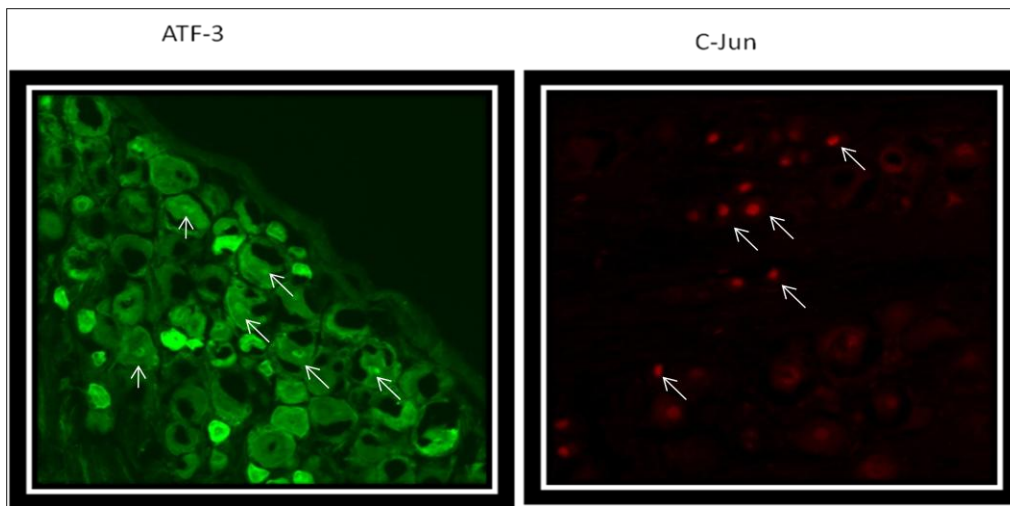


Figure 3.7 Positive Staining control: Ipsilateral L4/L5 DRGs 48 hours after sciatic nerve transection was stained with ATF-3 and c-Jun. Arrow indicates the positively stained cells.

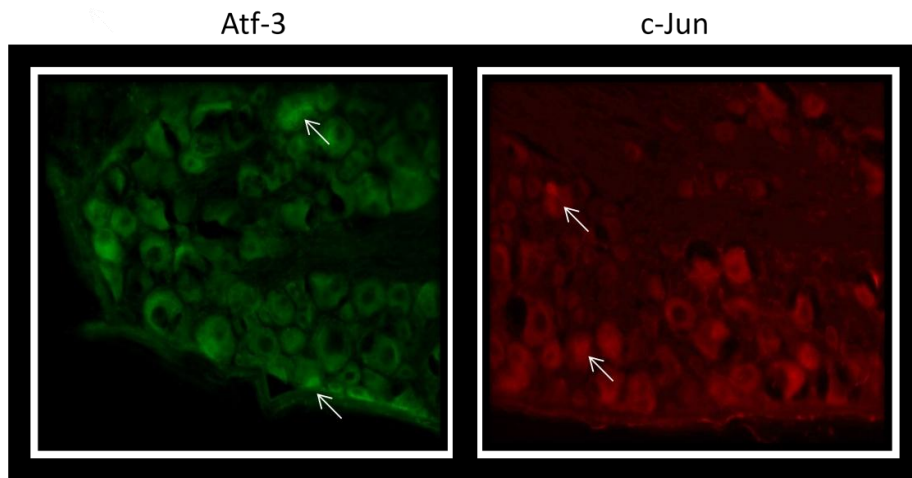


Figure 3.8 Minimum expression of ATF-3 and c-Jun was observed in ipsilateral L4/L5 DRGs of uninjured animals.

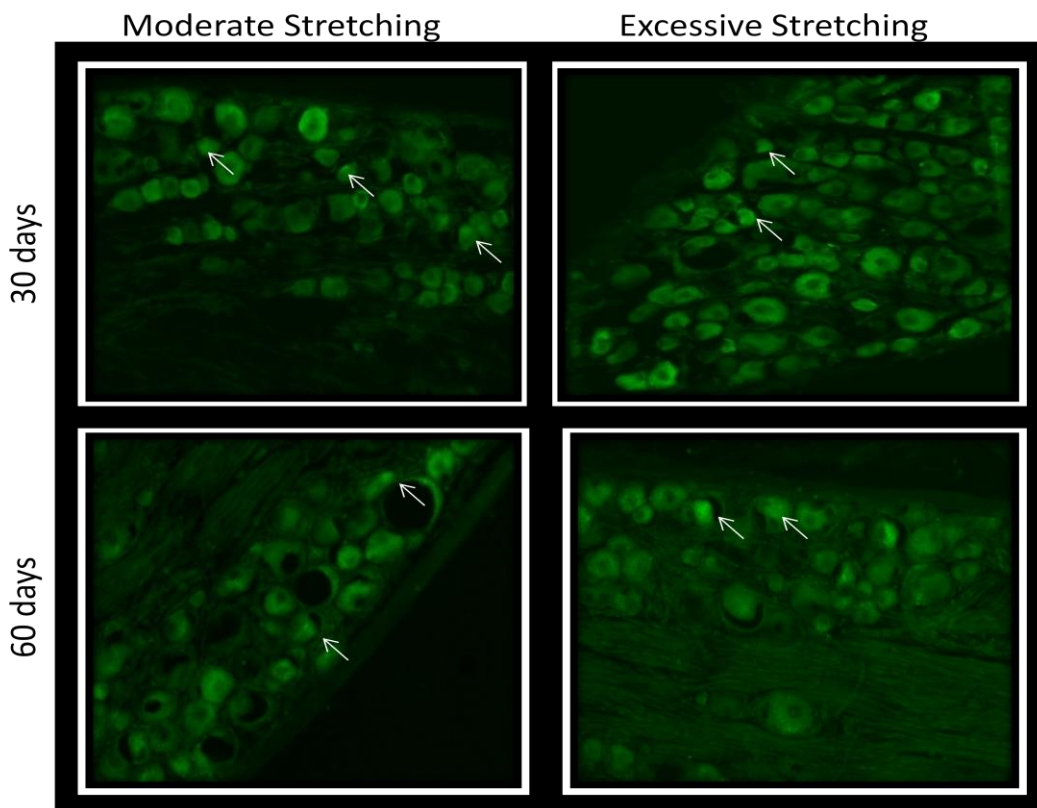


Figure 3.9 ATF-3 expression in ipsilateral L5 /L4 DRG with either moderate or excessive limb stretching at 30 days and 60 days after injury in REMI implanted acute injury animals. Arrow indicates Atf-3 stained DRGs. ATF-3 expression decreased significantly from 30 days to 60 days but was comparable between moderate stretching and excessive stretching at 30 days and 60 days respectively. (n=4, p<0.05)

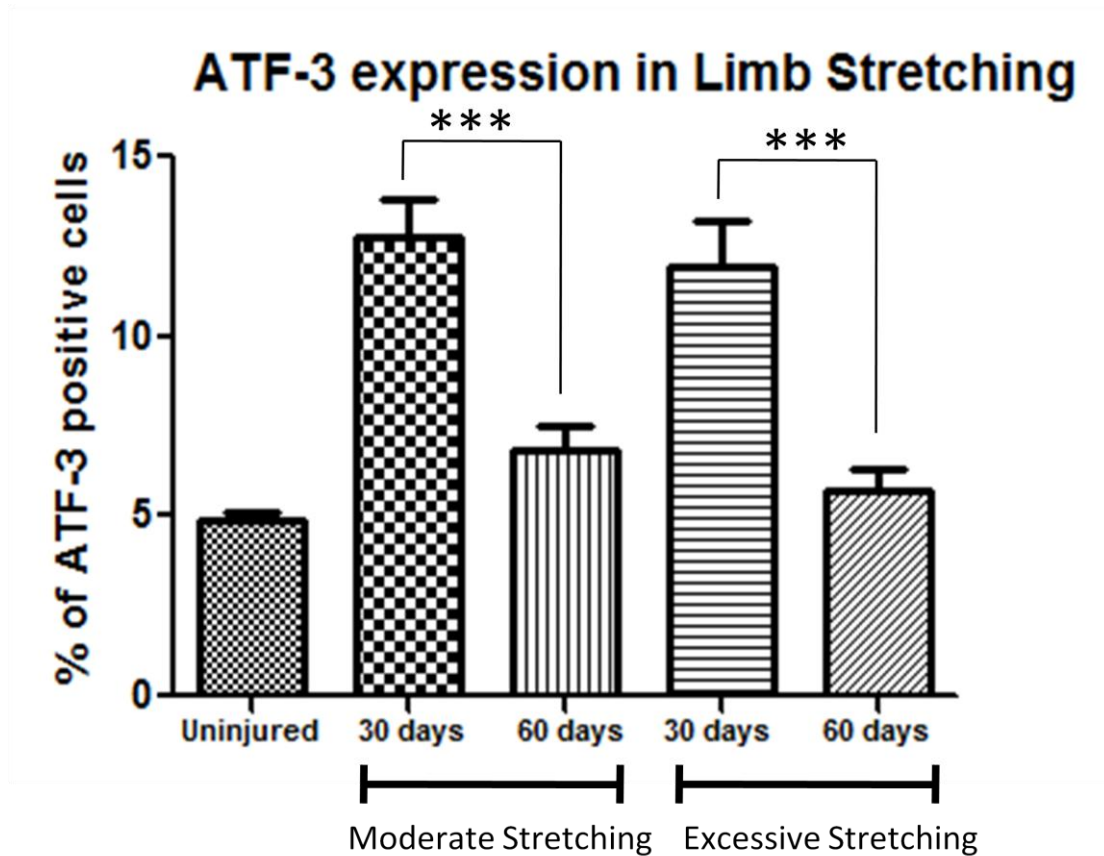


Figure 3.10 ATF-3 expression in ipsilateral L5 /L4 DRG with either Moderate Limb Stretching or Excessive Limb stretching at 30 days and 60 days after injury in REMI implanted acute injury animals. ATF-3 expression in ipsilateral L5 /L4 DRG decreased significantly with both moderate and excessive limb stretching at 30 days and 60 days after injury respectively. (n=4, One way ANOVA: $p < 0.05$)

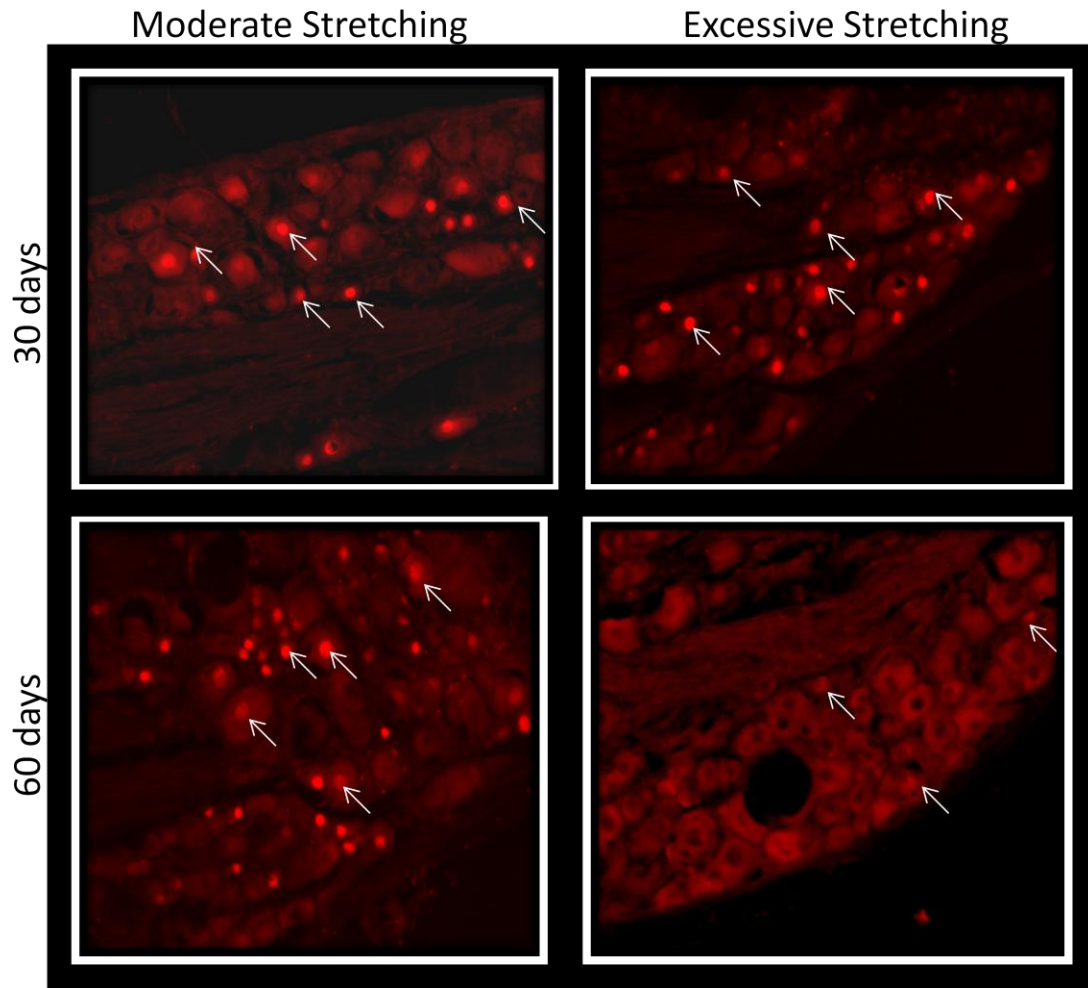


Figure 3.11 c-Jun expression in ipsilateral L5 /L4 DRG with either moderate or excessive limb stretching at 30 days and 60 days after injury in REMI implanted acute injury animals. Arrow indicates c-Jun stained DRGs. c-Jun expression in ipsilateral L4/L5 DRG with either moderate or excessive Limb stretching at 30 days and 60 days after injury. c-Jun expression decreased significantly from 30 days to 60 days at 100% stretching. (n=4, p<0.05)

c-Jun expression in Limb Stretching

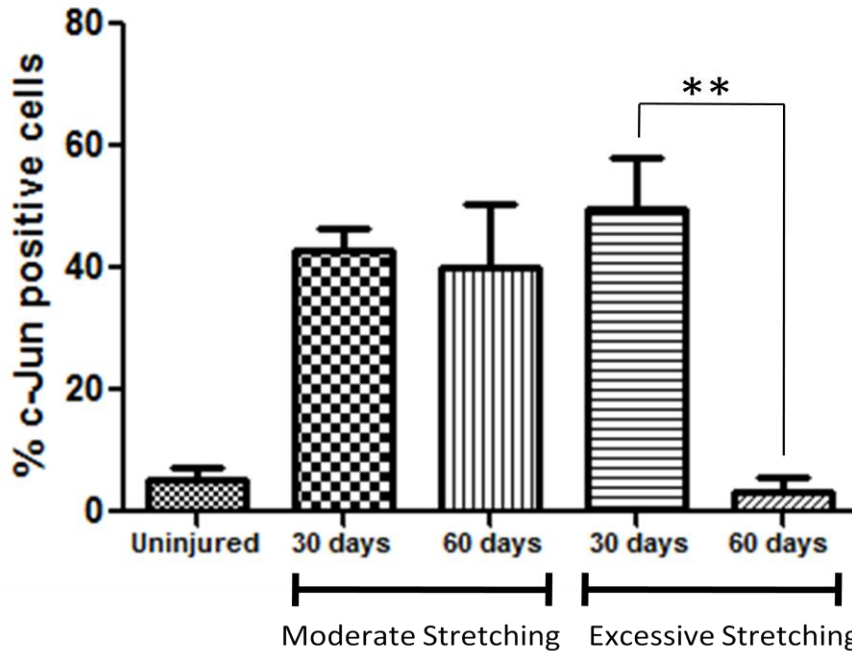


Figure 3.12 c-Jun expression in ipsilateral L5 /L4 DRG with either moderate or excessive Limb stretching at 30 days and 60 days after injury in REMI implanted acute injury animals c-Jun expression in ipsilateral L4 /L5 DRG decreased significantly at 60 days after injury with excessive stretching. (n=4; One way ANOVA: P<0.05)

3.3.1 Comparison between Nerve Stretching due to limb extension Vs No Stretching

Previously reported in an acute injury animal model, REMI neither create micro-injuries nor affect regeneration process in the sciatic nerve when REMI implanted animals were compared with empty polyurethane tubes implanted animals (Khobragade, 2011). The previous study was done by comparing the expression of ATF-3 and c-Jun at 15 days, 30 days and 60 days respectively (Fig 3.13)

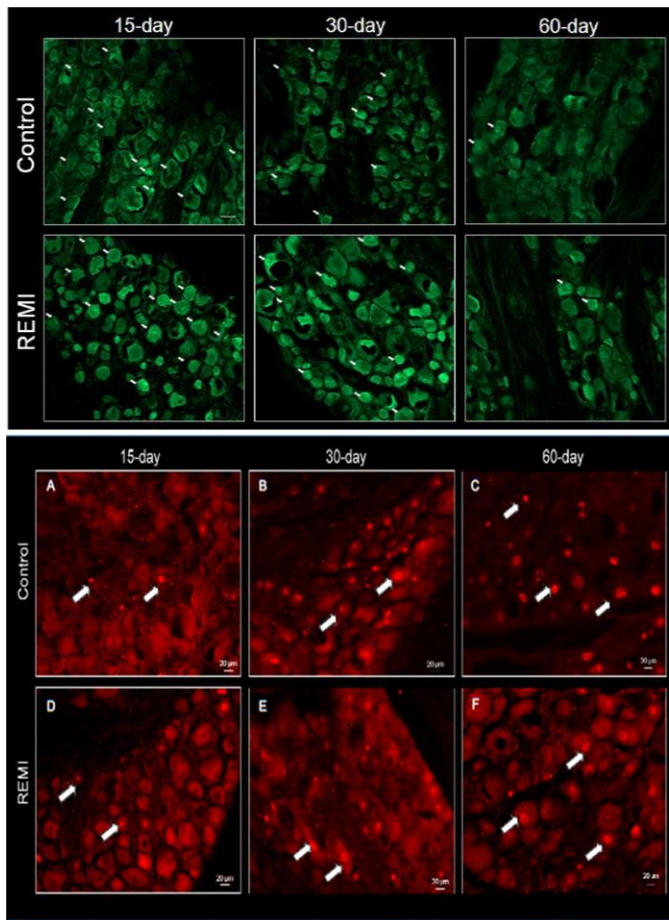


Figure 3.13 c-Jun expression in ipsilateral L5 /L4 DRG in acute injury without exercise at 15, 30 and 60 days after injury. ATF-3 and c-Jun expression was comparable between REMI implanted animals and control animals. Control animals were implanted with empty tube without REMI. c-Jun is in Red whereas ATF-3 is in green. (n=4; One way ANOVA: P<0.05) (Khobragade 2011)

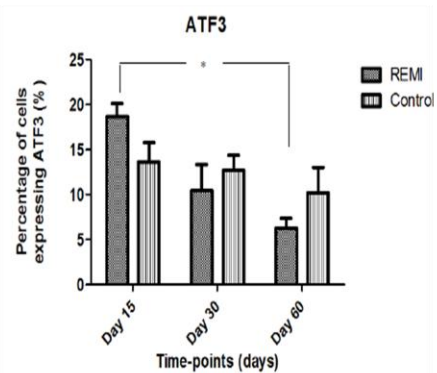
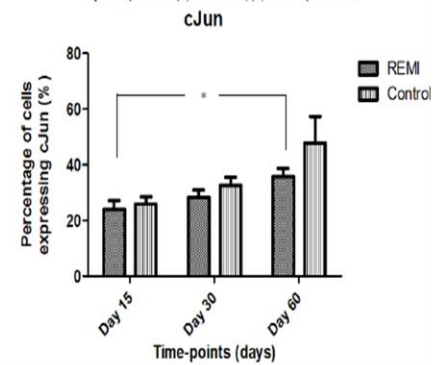


Figure 4.5 Comparison of percentage of L5 DRG cells expressing ATF3 after 15, 30 and 60 days of implantation (A) Control rats, (B) REMI implanted rats



Khobragade 2011

To test further the effects of nerve stretching, ATF-3 and c-Jun expression with either moderate or excessive nerve stretching were compared with previously reported acute injury without stretching. The comparisons of ATF-3 and c-Jun between nerve stretching and acute injury are shown in figure 3.14 and 3.15 respectively. ATF-3 expression of stretched animals (either moderate stretching or excessive stretching) was not significantly different compared to the unstretched animals at 30 days and 60 days after injury. c-Jun expression was not significant difference between stretched and unstretched animals besides excessive stretching

at 60 days after injury. However, c-Jun expression decreased significantly in excessive stretched animals compared to unstretched animals at 60 days after injury. As results, limb stretching neither induces micro-injury nor interferes with nerve regeneration when limb stretching is either moderate or excessive at 30 days after injury. Also, moderate limb stretching neither induce micro-injury not interfere with nerve regeneration at 60 days after injury. However, extensive limb stretching decrease nerve regeneration without inducing micro-injury at 60 days after injury.

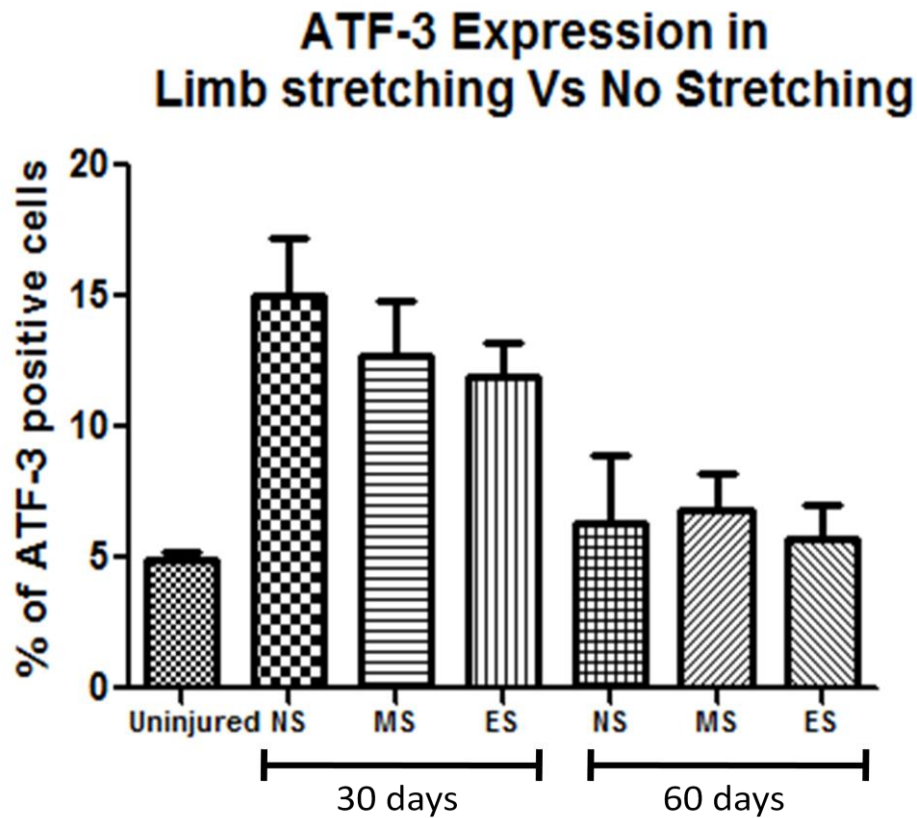


Figure 3.14 ATF-3 expression in ipsilateral L5 /L4 DRG of Stretched animals (either moderate or excessive) is not significantly different compared to unstretched animals. NS= No Stretching; MS= Moderate Stretching; ES: Excessive Stretching (n=4: One way ANOVA; p<0.05)

c-Jun expression in Limb Stretching Vs No-Stretching

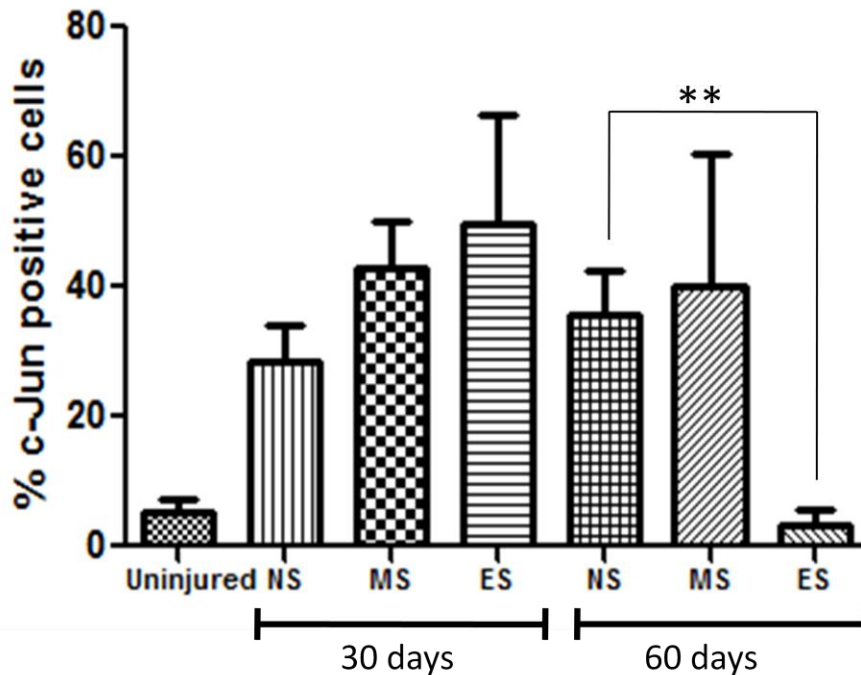


Figure 3.15 c-Jun expression in ipsilateral L5 /L4 DRG decreased significantly in excessive stretching animals compared to no stretching animals at 60 days after injury. No significant difference in ATF-3 is observed between unstretched and moderate stretched animals at both 30 days and 60 days after REMI implantation. NS = No Stretching; MS= Moderate Stretching; ES: Excessive Stretching (n=4; One way ANOVA; p<0.05)

3.4 Discussion

After nerve transection, the injured neurons switched from neuro-transmitter state to a pro-regenerative state in order to activate the regeneration-associated genes (Kiryu-Seo et. al. 2011, Arthur-Farraj et. al. 2012). ATF-3 is detected in DRG as early as 6-12 hours after axotomy and the intensity of signals increased to peak level 24 hours after axotomy (Tsuji no et. al. 2000, Linda et. al. 2011). As an early neuronal injury marker, the expression level of ATF-3 gradually decreased in a week or two (Tsuji no et. al. 2000, Linda et. al. 2011). Decreased level of ATF-3 from 30 days to 60 days in this study suggest that neither moderate stretching nor

excessive stretching of the limb, for 10 minutes at the rate of 20 mm/sec, induce REMI related tissue micro-injury.

Transcriptional factor, c-Jun governs the major aspects of the injury response and triggers regenerative program. It controls the expression of tropic factors, adhesion molecules, myelin clearance and the distinctive regenerative potential of peripheral nerves (Raivich et. al. 2004, Arthur-Farraj et. al. 2012). This study shows the percentage of c-Jun expression at 30 days after injury is not significantly different between unstretched and stretched animals with either moderate or excessive limb stretching. However, a significant difference is observed in c-Jun expression between unstretched and stretched animals at 60 days with excessive limb stretching but not with moderate limb stretching. This result suggests that neither moderate stretching nor excessive stretching affects nerve regeneration at 30 days after injury. However nerve regeneration significantly decreased overtime with excessive limb stretching. The significance of axonal regeneration is to replace the degenerated distal nerve segment thus, achieving target reinnervation and restitution of their functions (Allodi et. al. 2012). During regeneration-re-innervation period, activity-dependent therapies, like electrostimulation or exercise, positively influences neuromuscular and sensorimotor functional recovery after nerve injuries (Udina et. al. 2011). DRGs from exercised animals have shown to have higher level of BDNF, NT3 and GAP43 mRNAs than DRGs from sedentary animals (Molteni et. al. 2004). Also, exercise tends to decrease the level of myelin associate proteins and promotes neuronal outgrowth (Ghiani et. al. 2007). Previous study reported that moderate exercise for 1 hour/day, either active treadmill walking or passive cycling, improved muscle reinnervation, increased the number of regenerated axons in the distal nerve, and reduced the increased excitability of spinal reflexes after nerve lesion (Udina et. al. 2011). The histology of same study showed both passive and active exercise increased the number of myelinated axons in the distal tibial nerve, even above the normal number, 2 months after sciatic nerve lesion (Udina et. al. 2011). Primary sensory neurons decline c-Jun to basal levels after 4 to 6 weeks, when the peripheral

nerve stump successfully reinnervated to its target tissues (Herdegen et. al. 1998). Therefore, the intensity and the duration of limb stretching, 10min/day at 20 mm/sec for 60 days, applied in this study might have accelerated the axonal growth and target-reinnervation. Further studies, such as functional recovery test and muscles weight measurement, need to be done to validate if the excessive limb stretching applied in this experiment is actually attributed as the exercise for rapid regeneration of the nerve. It can be concluded that limb stretching neither induces REMI related micro-injury nor interfere with nerve regeneration at 30 days either with moderate or excessive limb stretching; however, it does decrease nerve regeneration might resulting target reinnervation if excessive stretching is applied till 60 days after injury.

CHAPTER 4

SPECIFIC AIM 2: EVALUATION OF MICRO-MOTION RELATED MICRO-INJURY AT REMI/PNS INTERFACE IN SUB-CHRONIC INJURY

4.1 Background

Replacing the missing limb with fully functional robotic prosthetic device is possible in amputees by direct interfacing the transected peripheral nerve to achieve motor control and closed loop sensory feedback (Garde et. al. 2009). After the transection of peripheral nerve, endoneurial Schwann cells and fibroblasts proliferate and migrate from both ends of the damaged nerve forming a bridge across the lesion site (Deumens et. al. 2010). When the regenerating axons fails to enter the distal endoneurial tubes, regenerative axons often form aberrant sprouting at the proximal nerve stump leading to the development of neuroma Fig 4.1 (Deumens et. al. 2010). Thus, distal stump and its target will suffer from atrophy. However, the residual nerves of amputee are still or can be brought back to be functional (Dhillon et. al. 2004).

Previously reported that REMI has successfully interfaced acute injury (REMI implant immediately after injury) as well as chronic injury (REMI implant 6 month after injury), however it suffered from signal loss overtime (Garde et. al. 2009, Seifert et. al. 2012). Mismatch of electrode-tissue elasticity, progressively damage the nerve, which eventually results in neuronal loss around the electrode as discussed in section 3.1. The function of interface in chronic models depends upon overtime tissue interaction. These tissue responses may have detrimental effects on the long term function of the electrode (Thelin et. al. 2012). Since peripheral nerve is intrinsically elastic, movement of interfaced nerve causes tissue micro-injury and interferes with regeneration in sub chronic injury model (REMI implantation 1 month after injury) is currently unknown. Therefore, this study evaluates if REMI induces tissue micro-

motion around the electrode, to cause micro-injury and to interfere with nerve regeneration, in a sub- chronic injury model.

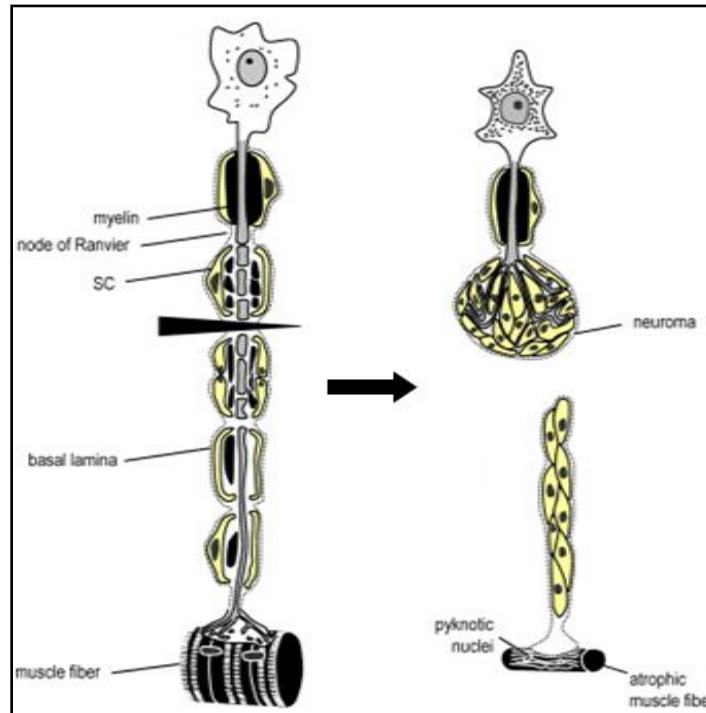


Figure 4.1 In the absence of distal segment, accumulations of growth cones undergo the formation of neuroma. (Deumens et. al. 2010)

4.2 Materials and Methods

FMA, placed in the polyurethane tube, was used to study regeneration and REMI induce micro-injury in sub-chronic injury model. FMA were custom made having the dimension of 2.45mm X 1.95 mm X 0.45 mm (Microprobes Inc. MD) and each FMA consists of 18 Platinum / Iridium (70 / 30 %) electrodes separated by 400 μ m and height range from 0.7 mm to 1 mm to maximize the neuronal contacts at different planes. Fifteen female Lewis adult rats (200-275g) were used in this study (n=3 for uninjured and n=12 for REMI implant respectively for three time points: 15 days, 30 days and 60 days).

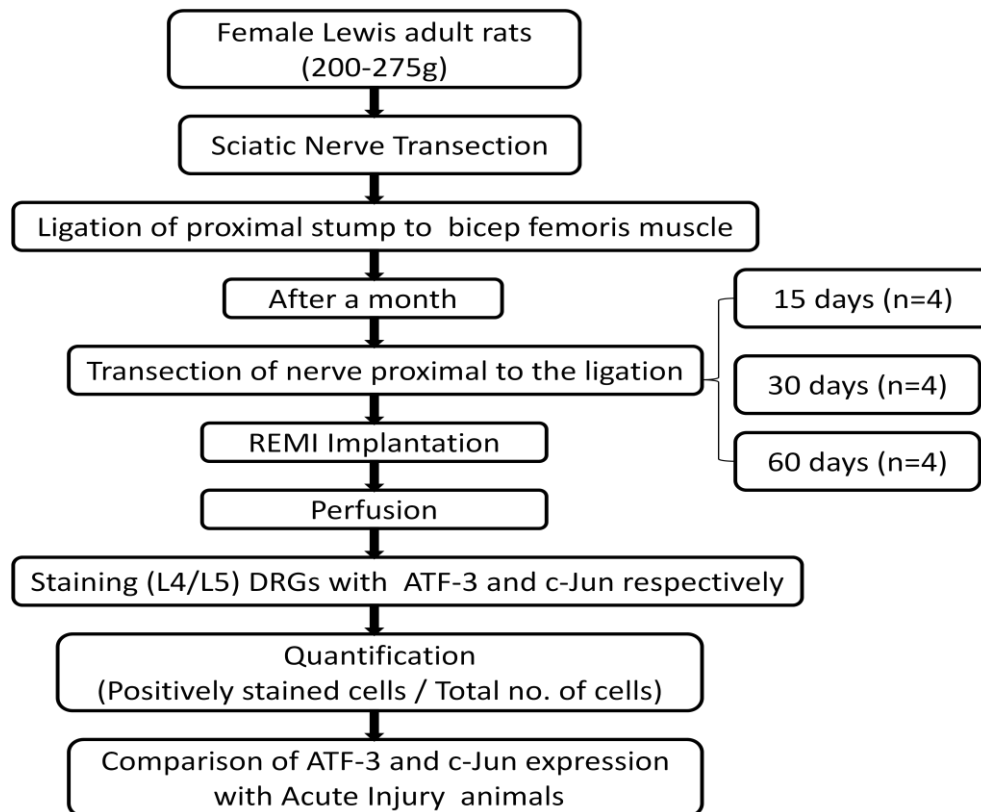


Figure 4.2 Experimental design of sub-chronic injury: Following the transection of sciatic nerve, proximal stump was sutured to the pectoral muscles. After a month, sciatic nerve was transected proximal to the first injury followed by REMI implantation. After 15 days, 30 days and 60 days of REMI implantation, animals were perfused and L4-L5 DRGs were stained with c-Jun or ATF-3.

4.2.1 Surgery and Implantation

The surgical environment and procedure were similar as described above in section 3.2 with some surgical modifications. The vertical incision was made on the left thigh then femoris and the semitendinosus muscles were separate apart. Sciatic nerve was exposed and transected. The proximal stump of the nerve endoneurium was sutured / ligated to the pectoral muscles using 10-0, 140 µm mono-filament. After a month, sciatic nerve proximal to the ligation was transected again. The nerve endoneurium was sutured using 10-0, 140 µm mono-filament after inserting the proximal and distal stumps of nerve in the ends of sterilized REMI conduit

respectively. The surgical procedures were carried out in accordance with the guidelines of Institutional Animal Care and Use Committee (IACUC) of the University of Texas, Arlington.

The animals were perfused 15 days, 30 days and 60 days after injury. Ipsilateral L4/L5 DRGs were extracted; immunofluorescence staining of Aft-3 and c-Jun, quantification and statistical analysis were done exactly the same way as described above in section 3.2.

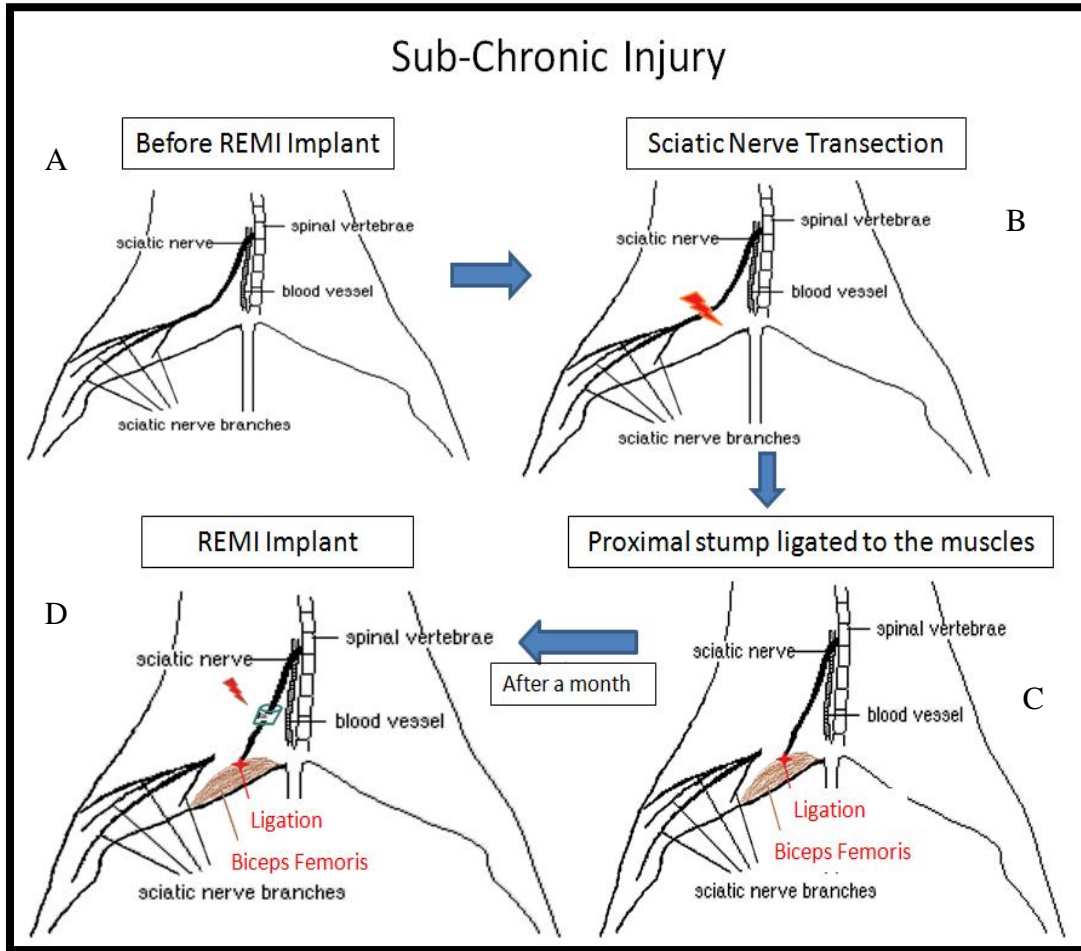


Figure 4.3 Procedure for sub-chronic injury. A) Sciatic nerve without the REMI implant. B) Sciatic Nerve is transected. C) Proximal stump of transected nerve is ligated to the biceps femoris muscles. D) Sciatic nerve undergoes second transection proximal to the first transection and REMI was implanted.

4.3 Results

After peripheral nerve transection, the regenerative associated genes are activated and controlled by the various transcription factors including ATF-3 and c-Jun. ATF-3 is unregulated

immediately after injury and is required to initiate the regenerative program whereas c-Jun regulate the generation. The Representative image, figure 4.4, shows the minimum expression of ATF-3 and c-Jun in ipsilateral L4/L5 DRGs of uninjured animals.

The representative image of ATF-3 labeled ipsilateral L4 /L5 DRGs of sub-chronic injury at 15 days 30 days and 60 days are shown in figure 4.5. The figure 4.5 shows the graph that compares the percentage expression of ATF-3 at 15 days, 30 days and 60 days after sub-chronic injury. ATF-3 expression in the DRGs neurons decreased significantly from 15 days ($18.71 \pm 3.4 \%$) to 30 days ($13.32 \pm 1.02\%$) to 60 days ($9.09 \pm 1.94 \%$).The representative image of c-Jun labeled ipsilateral L4 /L5 DRGs of sub-chronic injury at 15 days, 30 days and 60 days are shown in figure 4.7. The figure 4.8 shows the graph that compares the percentage expression of c-Jun expression at 15 days, 30 days and 60 days after sub-chronic injury. c-Jun expression increased significantly at 15 days (55.44 ± 8.29) and 30 days ($61.46 \pm 10.68\%$) as compared to 60 days ($44.55 \pm 2\%$).

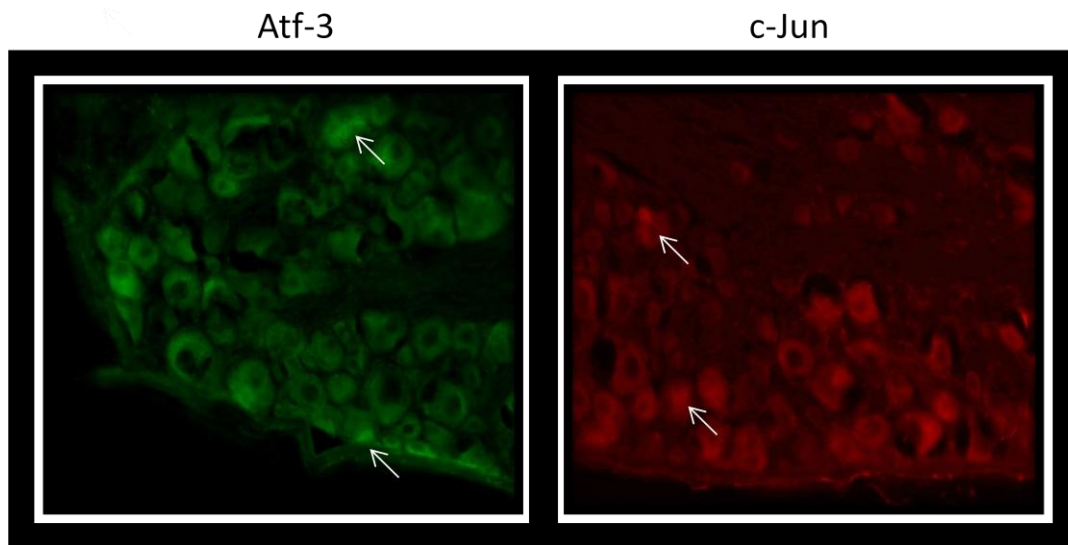


Figure 4.4 Minimum expression of ATF-3 and c-Jun was observed in ipsilateral L4/L5 DRGs of uninjured animals. Arrow indicates the positively stained cells.

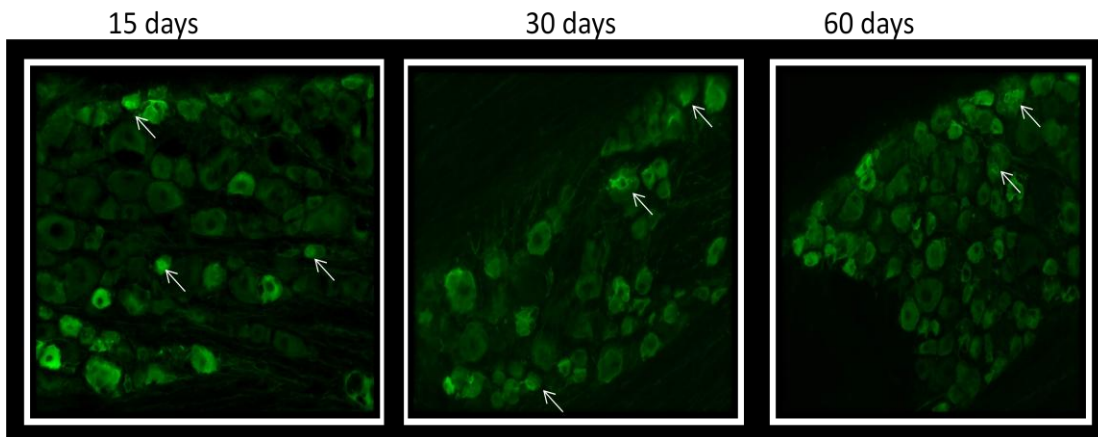


Figure 4.5 Atf-3 expression in ipsilateral L4/L5 DRGs in sub-chronically injured REMI implanted animals at 15 days, 30 days and 60 days. Arrows indicates the ATF-3 stained DRGs. ATF-3 decreased significantly from 15 days to 30 days to 60 days. (n=4, $p < 0.05$).

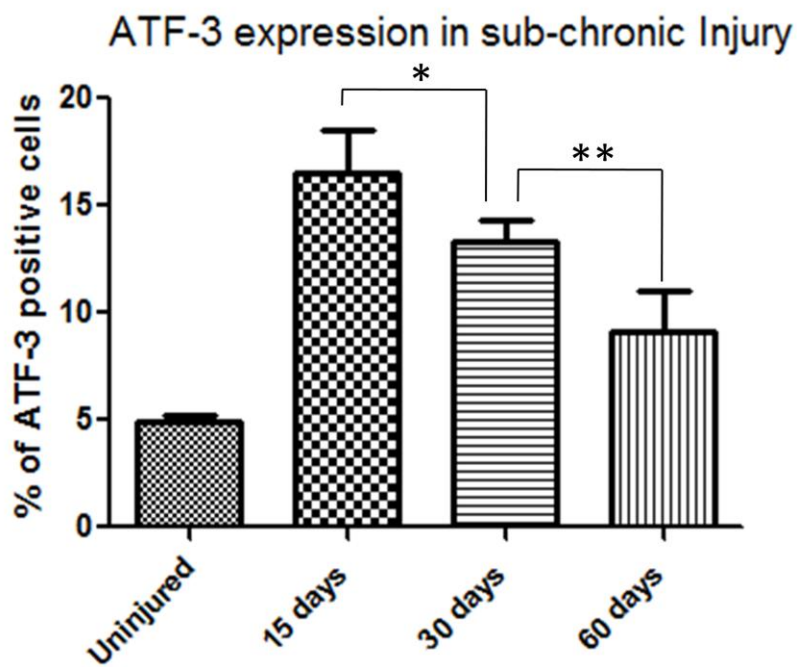


Figure 4.6 Atf-3 expressions in ipsilateral L4/L5 DRGs in sub-chronically injured REMI implanted animals at 15 days, 30 days and 60 days. The expression of ATF-3 in ipsilateral L5 /L4 DRGs decreased significantly from 15 days to 30 days to 60 days. (n=4, One way ANOVA; $p < 0.05$)

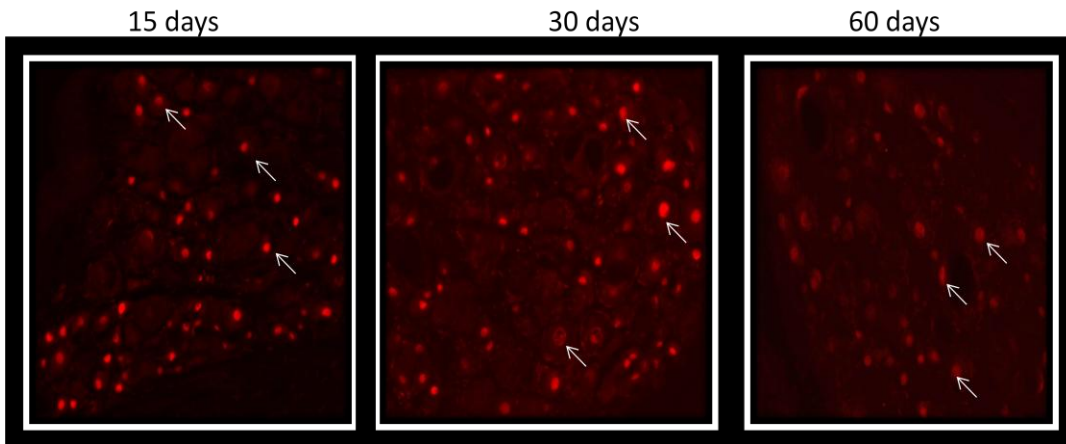


Figure 4.7 c-Jun expression in ipsilateral L4/L5 DRGs in sub-chronically injured REMI implanted animals at 15 days, 30 days and 60 days. Arrows indicates the c-Jun stained DRGs. c-Jun expression decreased significantly from 30 days to 60 days (n=4, p,0.05)

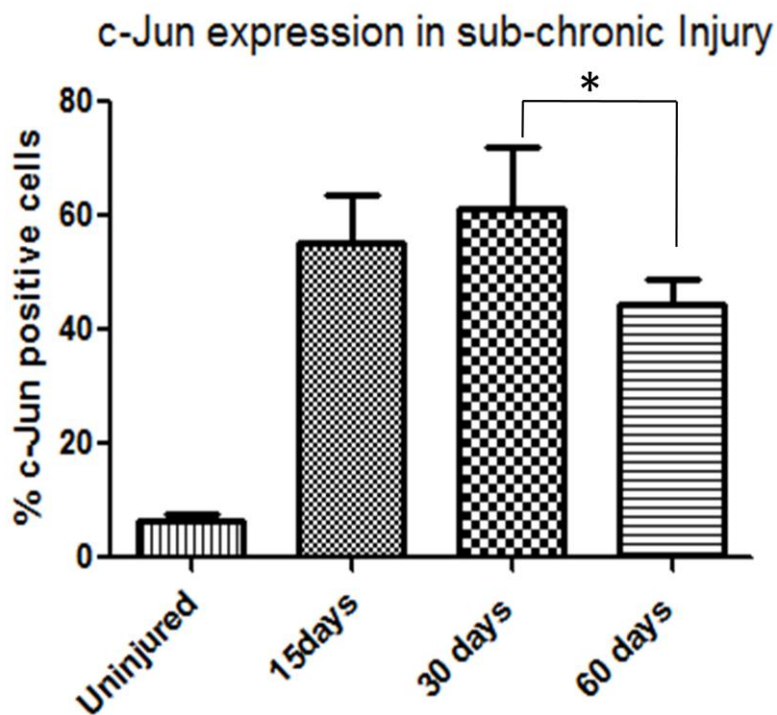


Figure 4.8 c-Jun expression in ipsilateral L4/L5 DRGs in sub-chronically injured REMI implanted animals at 15 days, 30 days and 60 days. c-Jun expression in ipsilateral L5 /L4 DRG decreased significantly from 30 days to 60 days. (n=4; One way ANOVA; p <0.05)

4.3.1 Comparison between Sub-chronic Vs Acute Injury

As previously reported REMI neither create micro-injuries nor affect regeneration process in the sciatic nerve, when REMI implanted animals were compared with empty polyurethane tubes implanted animals, in acute injury animals (Khobragade, 2011). The previous study was done by comparing the expression of Atf-3 and c-Jun in acute injury at 15 days, 30 days and 60 days respectively (Fig 3.13).

To further test the effect of REMI in sub-chronic injury animals, the expression of Atf-3 and c-Jun in sub-chronic injury animals were compared with acute injury animals as shown in figure in figure 4.9 and 4.10 respectively. Atf-3 expression in sub-chronic injury animals was not significantly different compared to the acute injury at 15 days, 30 days and 60 days respectively. The expression of c-Jun increased significantly at 15 days and 30 days in sub-chronic injury compared to acute injury. However, the c-Jun expression in sub-chronic injury animals was comparable to acute injury animals at 60 days. The results suggest that REMI doesn't induce tissue micro-injury at 15 days, 30 days and 60 days after injury. However the nerve regeneration increased receiving the second nerve transection. This provide evidence that REMI implant forms a stable interface with nerve and are not affected by tissue micro-motion

ATF-3 expression in Acute Injury Vs Sub-Chronic Injury

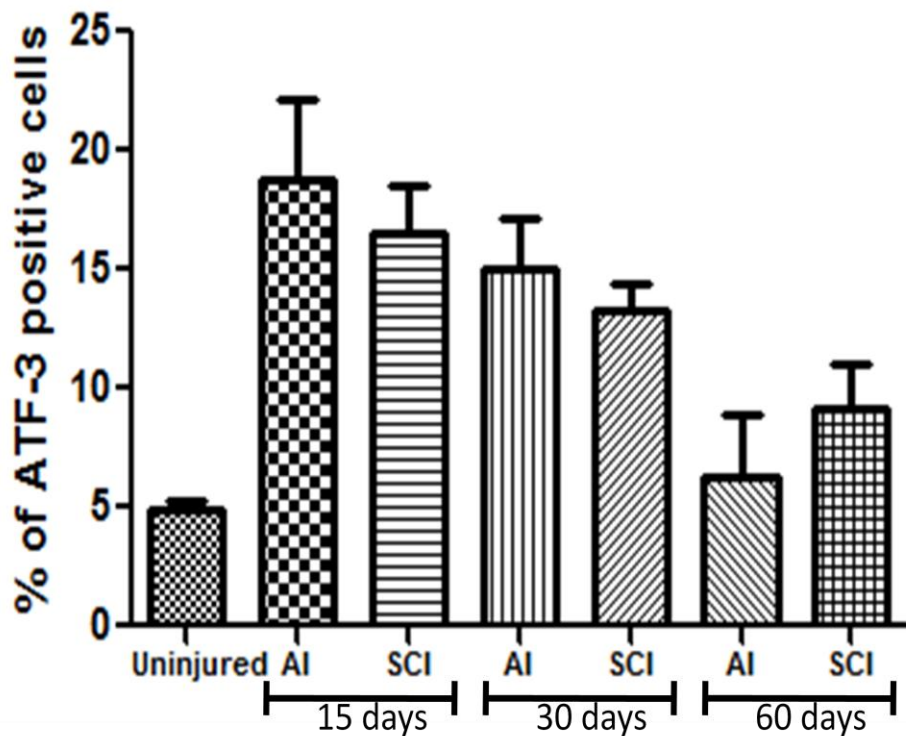


Figure 4.9 The percentage of ATF-3 expression in ipsilateral L5 /L4 DRG of Sub-chronic injury is not significantly different compared to acute injury at 15 days, 30 days and 60 days respectively. AI = Acute injury; SCI: Sub-Chronic Injury (n=4; One way ANOVA; $p < 0.05$)

c-Jun expression in Acute Injury Vs Sub-Chronic Injury

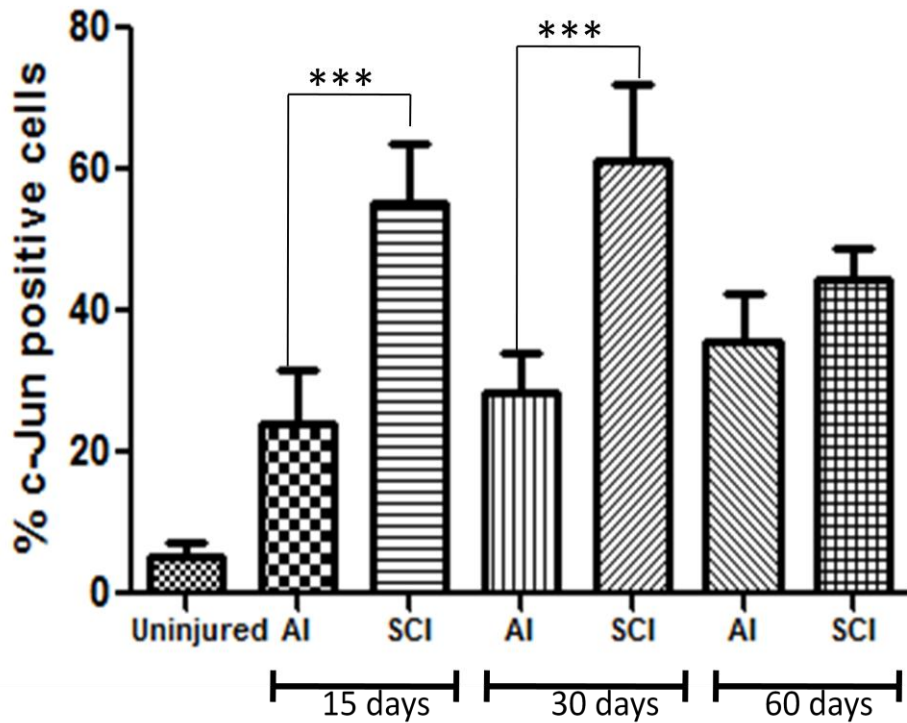


Figure 4.10 The percentage of c-Jun expression in ipsilateral L5 /L4 DRG of Sub-chronic injury increased significantly at 15 days and 30 days compared to acute injury. No significant difference is observed between acute injury and sub-chronic injury at 60 days after REMI implantation. AI = Acute Injury; SCI = Sub-Chronic Injury (n=4; One way ANOVA; p<0.05)

4.4 Discussion

After injury, axons distal to the lesion sites are disconnected from the neuronal body and degenerate, leading to denervation of the peripheral organs (Allodi et. al. 2012, Udina et. al. 2011). The wallerian degeneration creates a micro-environment distal to the injury site while neuronal body switches its function and activates the transcriptional factors to promote axonal re-growth and regeneration. Transcriptional factor ATF-3 is upregulated immediately after injury to induce the nerve regeneration process, which gradually decreased in week or 2 as discussed

in section 2.4. No significant difference in the expression of ATF-3 was observed between sub-chronic and acute injury. Moreover, ATF-3 significantly decreased from 15 days to 30 days to 60 days in sub-chronic injury suggesting that REMI does not induce micro-injury due to tissue micro-motion.

As a regenerative marker, expression of c-Jun is persistent throughout the regeneration process after axotomy. Previously, it has been reported that peripheral neuron switches to a regenerative state after axotomy (Allodi et. al. 2012). Thus, it will regenerate faster after receiving the second injury if the second injury is applied during regenerative state of neurons (Allodi et. al. 2012). In this study, expression of c-Jun was significantly higher in sub-chronic injury animals at 15 days and 30 days compared to acute injury. Since, sub-chronic injury animals received second transection after a month of initial transection, the first injury primed the neurons to switch into the regenerative state and second injury might have accelerates the regeneration program. However, the c-Jun expression in sub-chronic injury animals was comparable to the acute injury animals at 60 days. This suggests that non-obstructive regenerative multi-electrode arrays can guide nerve regeneration in close proximity to their target, providing relatively stable neurointerfacing to sub-chronic injured peripheral nerves.

CHAPTER 5

CONCLUSION AND FUTURE WORK

Peripheral Nerve Interface holds a promising technology for a wide range of neuroprosthetic applications. The emergence of silicon micro-fabrication technique has yielded increasingly smaller and higher electrode count devices that are capable of recording from greater volumes of neural tissue and with improved spatial discrimination (Biran et. al. 2005). However, current technology has been suffered from the inconsistency performance in the long term application. Recently developed REMI has shown to be capable of recording as early as 8 days but have also been suffered from signal decay overtime (Seifert et. al. 2012). Instability of electrode at tissue interface induces neuronal micro-injury which contributes to the inflammatory response at the injury site. Previous studies has reported that encapsulation layers of fibroblasts, macrophages, and reactive astrocytes surrounds implanted electrodes eventually insulating the electrodes from nearby neurons (Brain et. al. 2007) Eventually such responses reduce the neurons at the interface leading to increase the distance between electrode and neurons. Decreased in ATF-3 expression from 30 days to 60 days in acute injury with or without stretching in this study suggests that REMI implant do not induce tissue micro-injury. Results were consistency with sub-chronic injury models.

During the first week of nerve transection, peripheral nerve undergo significant remodeling process to achieve successful regeneration which will be achieved by interactions between the neurons and the neighboring Schwann cells and also by the interaction of different adhesion molecules and their receptors and several tropic factors (Kiryu-Seo, S., Kiyama, H. 2011). The expression of c-Jun was consistent overtime with moderate stretching in acute injury model, however, decreased overtime with excessive stretching. This result suggests that REMI does not alter regeneration process; however excessive stretching may have elicited axonal

regeneration. Primary sensory neuron declines c-Jun expression to basal level after 4 to 6 weeks, when peripheral nerve stump successfully reinnervated to its target tissues (Herdegen et. al. 1998). Previous study reported that moderate exercise for 1 hour / day, either active treadmill walking or passive cycling, improved muscle reinnervation, increased the number of regenerated axons in the distal nerve, and reduced the increased excitability of spinal reflexes after nerve lesion (Udina et. al. 2011). The histology of same study showed both passive and active exercise increased the number of myelinated axons in the distal tibial nerve, above the normal, 2 months after sciatic nerve lesion (Udina et. al. 2011). DRGs from exercised animals have shown to have higher level of BDNF, NT3 and GAP43 mRNAs than DRGs from sedentary animals (Molteni et. al. 2004). Previous characterization of the stretch injury in the peripheral nerve has reported that nerve will ruptured after receiving 40% nerve strain whereas conduction velocity deficits after 10-15% strain (Kwan et.al.1992). The nerve stretching has been measured previously by Watson 2012 in our lab has shown that moderate limb extension will generate 18% strain and excessive limb extension will generate 34% strain (Watson 2012). Therefore, the strain applied to the nerve with excessive limb stretching does not seem to be causing nerve damage. This finding is also supported by the previous study in the lab reported by Watson 2012. The electrophysiology results showed no increase in the rate of signal loss among either of the stretching groups compared to the control group till 30 days after injury as reported previously by Watson in our lab (Watson 2012). There was no statistical difference between the average numbers of spiking units with respect to limb stretching (Watson 2012). Moreover, the numbers of regenerating axons were comparable between unstretched and excessive stretched animals at 60 days after REMI implantation (Watson 2012). Stretching might have increased the release of trophic factor to act on regenerating axons and to increase central neuroplasticity by intracellular pathways. Therefore, it can be concluded that excessive stretching attributed as an exercise training accelerating axonal outgrowth, and target reinnervation. The unexpected finding in the results of excessive stretching may be explained by known beneficial effect of

exercise in nerve regeneration, however further studies such as functional recovery test, regenerative axonal counts, muscles weight need to be perform to validate the statement.

Quantitative expression of c-Jun in sub-chronic injury was increased at 15 days and 30 days but was comparable to acute injury at 60 days. The mechanism behind the increase in nerve regeneration at earlier phase of sub-chronic injury is currently unknown. However, previously it has been reported that the first injury primed the neurons to switch into the regenerative state and thus second injury, during the regenerative state of neuron, accelerates the regeneration program (Allodi et. al. 2012). Previously reported regeneration rostral to a lesion can be achieved provided the intrinsic growth capacity of the injured neurons is sustained by repeated priming (Neumann et. al. 2005). Intrinsic growth capacity is enhanced by the priming peripheral nerve lesion but the postinjury lesion of the sciatic nerve sustained growth capacity before the scar barrier was fully established (Neumann et. al. 2005). Once primary sensory neurons are primed by peripheral axonal injury, they grow more rapidly in response to a subsequent lesion, in what has become known as the conditioning effect (Seiffers et. al. 2007).

The subjects in the sub-chronic injury model had undergone through two times transection of sciatic nerve, the first transection might have primed the neurons to switch into the regenerative state and thus second transection after a month, might have accelerates the regeneration program. Further study need to be done to illustrate the underlying mechanism including the comparison of sub-chronic injury with or without REMI implantation. Besides ATF-3 and c-Jun, other well studies regenerative markers such as STAT3 could be used to validate the nerve micro-injury and regeneration. Retrograde transfer of STAT3 acts as the positive injury signal to soma and regulates gene transcription binding with other transcriptional factors (Kiryu-Seo et. al. 2011). From these results it can be concluded that REMI doesn't alter nerve regeneration in acute as well as sub-chronic injury model.

REMI do not induce micro-motion related micro-injury as shown by ATF-3 and c-Jun thus is not responsible for signal decay overtime. Previously reported animals exhibiting spike

activity increased from 29% to 57% from 7 to 14 days following REMI implantation (Seifert et. al. 2012). Also two weeks after REMI implantation, numbers of neurofilament-positive axons in the control and REMI implanted nerves were comparable, and in both cases the number of myelinated axons was low (Seifert et. al. 2012). Remyelination initiates 2–3 weeks after the initial injury in peripheral nerve (Le beau 1987). During nerve regeneration, myelin layers wrap around the myelinating axons resulting in the formation of insulating sheath. Myelin possesses high electrical resistance and low capacitance thus acts as insulator around axons (Le beau 1987). Therefore, myelination might be a cause of signal decay overtime but further study need to be done. As the conclusion, non-obstructive Regenerative Multi-Electrode Array can guide regenerative axons in the close proximity to their target providing relatively stable peripheral neurointerfacing to an acute injury and also to sub-chronic injury via the formation of a nerve/electrode array monolithic structure resulting from the fibrotic encapsulation of the implant.

REFERENCES

- Allodi, I., Udina, E., Navarro, X. Specificity of peripheral nerve regeneration: Interactions at the axon level. *Progress in Neurobiology*. 2012. 98: 16–37
- Aoyagi, Y., Stein, R. B., Branner, A., Pearson, K. G., Normann, R. A. Capabilities of a penetrating microelectrode array for recording single units in dorsal root ganglia of the cat. *Journal of Neuroscience Methods*. 2003. 128: 9-20
- Arthur-Farraj, P.J. and et.al. c-Jun Reprograms Schwann Cells of Injured Nerves to Generate a Repair Cell Essential for Regeneration. *Neuron*. 2012. 75: 633–647
- Bandara, D.S.V., Gopura, R.A.R.C., Hemapala, K.T.M.U. and Kiguchi, K. Upper extremity prosthetics: current status, challenges and future directions. *The Seventeenth International Symposium on Artificial Life and Robotics*. 2012. 875-880
- Behrend, C., Reizner, W., Marchessault, J.A., Hammert, W.C. Update on Advances in Upper Extremity Prosthetics. *Journal of Hand Surgery*. 2011. 36A:1711–1717
- Ben-Yaakov, K. , Dagan, S.Y., Segal-Ruder, Y., Shalem, O., Vuppalachchi, D., Willis, D.E., Yudin, D., Rishal, I., Rother, F., Bader, M., Blesch, A., Pilpel, Y., Twiss, J.L., Fainzilber, M. Axonal transcription factors signal retrogradely in lesioned peripheral nerve. *EMBO Journal*. 2012. 31:1350–1363
- Billock, J. N. Hands versus Hooks. *Clinical prosthetics and Orthotics*. 1986. 10 (2): 57-65
- Biran, R., Martin, D.C., Tresco, P.A. Neuronal cell loss accompanies the brain tissue response to chronically implanted silicon microelectrode arrays. *Experimental Neurology*. 2005. 195: 115 – 126
- Biran, R., Martin, D.C., Tresco, P.A. The brain tissue response to implanted silicon microelectrode arrays is increased when the device is tethered to the skull. *Journal of Biomedical Materials Research Part A*. 2007. 82A(1): 169-178
- Boretius, T., Bardia, J., Pascual-Font, A., Schuettler, M., Navarro, X., Yoshida, K., Stieglitz, T. A transverse intrafascicular multichannel electrode (TIME) to interface with the peripheral nerve. *Biosense Bioelectron*. 2010. 26 (1): 62-9
- Bowman, B.R., Erickson, R. C. Acute and chronic implantation of coiled wire intraneural electrodes during cyclical electrical stimulation. *Ann Biomed Eng*. 1985.13(1):75-93.
- Branner, A., Stein, R. B., Fernandez, E., Aoyagi, Y., Normann, R. A. Long-term stimulation and recording with a penetrating microelectrode array in cat sciatic nerve. *IEEE Transactions Biomed Eng*. 2004. 51(1):146-57

- Brück, W. The role of macrophages in Wallerian degeneration. 1997. *Brain Pathol* 7:741-752
- Bunge, M.B., Williams, A.K., Wood, P.M. Neuron-Schwann cell interaction in basal lamina formation. *Developmental Biology*. 1982. 92 (2), 449–460
- Chen, Z-L., Yu, W-M, and Strickland, S. Peripheral Regeneration. *Annual Review Neuroscience*. 2007. 30: 209–33
- Cheung K. Thin-Film Microelectrode Arrays for Biomedical Applications. *Implantable Neural Prosthesis 2: Biological and Medical Physics, Biomedical Engineering*. 2010. 157-190.
- Cosker, K.E., Courchesne, S. L. and Segal, R.A. Action in the axon: generation and transport of signaling endosomes. 2008. 18 (3): 270-275
- Cravioto, H., Battista, A. Clinical and ultrastructural study of painful neuroma. *Neurosurgery*. 1981. 8(2):181-90
- Deumens, R., Bozkurt, A., Meek, M.F., Marcus, M.A.E., Josten, E.A.J., Weis, J., Brook, G.A. Repairing injured peripheral nerves: Bridging the gap. *Progress in Neurobiology*. 2010. 92 (3): 245-276
- Dhillon, G.S., Lawrence, S.M., Hutchinson, D.T., Horch, K.W. Residual function in peripheral nerve stumps of amputees: implications for neural control of artificial limbs. *Journal of Hand Surgery*. 2004. 29(4):605-15
- Doeringer, J.A and Hogan, N. Performance of Above Elbow Body-Powered Prosthesis in Visually Guided Unconstrained Motion Tasks. *IEEE transactions of Biomedical Engineering*. 1995. 42(6): 621-631
- Donoghue, J.P. Connecting cortex to machines: recent advances in brain interfaces. *Nature Neuroscience supplement*. 2002. 5: 1085-1088
- Fillauer Orthotics & Prosthetics, Inc. Chattanooga, TN. *Mechanical Hooks*: 2012
- Fisher, L.E., Tyler, D.L., Triolo, R.J. Chronic stability and selectivity of four-contact spiral nerve-cuff electrodes in stimulating the human femoral nerves. *Journal of Neural Engineering*. 2009. 6(4)
- Fried, K., Govrin-Lippmann, R., Rosenthal, F., Ellisman, M.H., Devor, M. Ultrastructure of afferent axon endings in neuroma. *J. Neurocytology*. 1991. 20: 682–701
- Fu, Sy and Godon, T. The cellular and molecular basis of peripheral nerve regeneration. *Molecular Neurobiology*. 1997. 14(1-2):67-116

Garde, K., Keefer, E., Botterman, B., Galvan, P., Romero, M.I. Early interfaced neural activity from chronic amputated nerves. *Frontiers in Neuroengineering*. 2009

Gaudet, A. D, Popovich, P.G. and Ramer. M. S. Wallerian degeneration: gaining perspective on inflammatory events after peripheral nerve injury. *Journal of Neuroinflammation*. 2011. 8 (110): 1-13

Gaunt, R.A., Hokanson, J.A., Weber, D.J. Microstimulation of primary afferent neurons in the L7 dorsal root ganglia using multielectrode arrays in anesthetized cats: thresholds and recruitment properties. *J Neural Eng*. 2009. 6(5)

Ghiani, C.A., Ying, Z., de Vellis, J., Gomez-Pinilla, F. Exercise decreases myelin associated glycoprotein expression in the spinal cord and positively modulates neuronal growth. *Glia*. 2007. 55, 966–975

Gold, B.G. Axonal regeneration of sensory nerves is delayed by continuous intrathecal infusion of nerve growth factor. *Neuroscience*. 1997. 76: 1153–1158

Gonenli, I., Celik-Butler, Z. and Butler, D. Surface Micromachined MEMS Accelerometers on Flexible Polyimide Substrate. *Sensors Journal, IEEE*. 2011. 1-1

Goodall, E. V., Lefurge, T. and Horch, K. Information contained in sensory nerve recordings made with intrafascicular electrodes. *Biomedical Engineering, IEEE Transactions*. 1991. 38 (9): 846-850

Harvey, Z. T., Potter, M. B. K., Vandersea, J., Wolf, E. Prosthetic Advances. *Journal of surgical orthopedic advances*. 2012. 21(1): 58-64

Herdegen, T., Skene, P., and Bahr, M. The c-Jun transcription factor–bipotential mediator of neuronal death, survival and regeneration. *Trends Neuroscience*. 1997. 20: 227–231

Herdegen, T. and Leah, J.D. Inducible and constitutive transcription factors in the mammalian nervous system: control of gene expression by Jun, Fos and Krox, and CREB / ATF proteins. *Brain Research Review*. 1998. 28: 370–490

Hochberg, L. R., Serruya, M. D., Friehs, G. M., Mukand, J. A., Saleh, M., Caplan, A. H., Branner, A., Chen, D., Penn, R. D., Donoghue, J. P. Neuronal ensemble control of prosthetic devices by a human with tetraplegia. *Nature*. 2006. 442: 164-171

Hochberg, L.R., Bacher, D., Jarosiewicz, B., Masse, N. Y., Simeral, J. D., Vogel, J., Haddadin, S., Liu, J., Cash, S.S., Smagt, P.V.D., Donoghue, J.P. Reach and grasp by people with tetraplegia using a neurally controlled robotic arm. *Nature*. 2012. 485: 372-374

- Huber, A.B., Kolodkin, A.L., Ginty, D.D., Cloutier, J.F. Signaling at the growth cone: ligand-receptor complexes and the control of axon growth and guidance. *Annual Review of Neuroscience*. 2003. 26, 509–563
- Hyatt, S. H., Schreiber, R. C., Shoemaker, S.E., Sabe, A., Reed, E., Zigmond, R. E. Activating transcription factor 3 induction in sympathetic neurons after axotomy: response to decreased neurotrophin availability. *Neuroscience*. 2007. 150 (4):887-97
- Ide, C. Peripheral nerve regeneration. *Neuroscience Research*. 1996. 25: 101-121
- Kenney, A. M. and Kocsis, J. D. Peripheral axotomy induces long term c-Jun amino-terminal kinase-1 activation and activator protein-1 binding activity by c-Jun and JunD in adult rat dorsal root ganglia in vivo. *J. Neurosci*. 1998. 18:1318–1328
- Khobragade, Nivedita, M.S. Micromotion and scarring does not contribute to failure of regenerative peripheral neural interfacing . 2011. University of Texas, Arlington
- Kim, Y.T. and Romero-Ortega, M.I. Material considerations for peripheral nerve interfacing. *Materials Research Society Bulletin*. 2012. 37: 1-8
- Kiryu-Seo, S., Kato, R., Ogawa, T., Nakagomi, S., Nagata, K., and Kiyama, H. Neuronal Injury-inducible Gene Is Synergistically Regulated by ATF3, c-Jun, and STAT3 through the Interaction with Sp1 in Damaged Neurons. *Journal of biological chemistry*. 2008. 283 (11): 1-9
- Kiryu-Seo, S., Kiyama, H. The nuclear events guiding successful nerve regeneration. *Frontiers in Molecular Neuroscience*. 2011. 4 (53): 1-11
- Kuiken, T.A., Li, G., Lock, B. A., Lipschutz, R. D., Miller, L. A., Stubblefield, K.A., Englehart, K. B. Targeted Muscle Reinnervation for Real-time Myoelectric Control of Multifunction Artificial Arms. *The Journal of American Medical Association*. 2009. 301(6):619-628
- Kwan, M. K., Wall, E. J., Massie, J., Garfin, S. R. Strain, stress and stretch of peripheral nerve Rabbit experiments in vitro and in vivo. *Acta Orthop Scand*. 1992. 63 (3): 267-272
- Lago, N., Udina, E., Ramachandran, A., and Navarro, X. Neurobiological Assessment of Regenerative Electrodes for Bidirectional Interfacing Injured Peripheral Nerves. 2007. *IEEE Transactions Biomed Eng*. 54 (6): 1130-1137
- Lawrence, S. M., Dhillon, G.S., Horch, K.W. Fabrication and characteristics of an implantable, polymer-based, intrafascicular electrode. *Journal of Neuroscience Methods*. 2003. 131 (1-2): 9-26
- Lee, H., Bellamkonda, R. V., Sun, W. & Levenston, M. E. Biomechanical analysis of silicon microelectrode-induced strain in the brain. *Journal of Neural Engineering*. 2005. 2, 81.

Le Beau, J. M. Powell, H. C. and Ellisman, M. H. Node of Ranvier formation along fibres regenerating through silicone tube implants: A freeze-fracture and thin-section electron microscopic study," J. Neurocytol. 1987. 16(3): 347–358

Lebedev, M. A. and Nicolelis, M. A. L. Brain–machine interfaces: past, present and future. Trends in Neurosciences. 2006. 29(9): 536-546

Lebedev, M. A., Tate, A. J., Hanson, T. L., Li, Z., O'Doherty, J. E., Winans, J. A., Ifft, P. J., Zhuang, K. Z., Fitzsimmons, N. A., Schwarz, D. A., Fuller, A. M., An, J. H., Nicolelis, M. A. Future developments in brain-machine interface research. 2011. Clinics. 66 (S1): 25-32

Lefurge T, Goodall E, Horch K, Stensaas L, Schoenberg A. Chronically implanted intrafascicular recording electrodes. Ann Biomed Eng 1991. 19:197–207.

Liberating Technologies, Inc. Holliston, MA. Mechanical Hands: 2012

Linda, H., Skold, M.K., Ochsmann, T. Activating transcription factor 3, a useful marker for regenerative response after nerve root injury. Frontiers in Neurology: Neurotrauma. 2011. 2(30)

Lindwall, C., Dahlin, L., Lundborg, G., and Kanje, M. Inhibition of c-Jun phosphorylation reduces axonal outgrowth of adult rat nodose ganglia and dorsal root ganglia sensory neurons. Mol.Cell. Neurosci. 2004. 27: 267–279

Loeb, G. E., Peck, R. A. Cuff electrodes for chronic stimulation and recording of peripheral nerve. J Neurosci Methods 1996. 64:95–103

Lofti, P., Garde, K., Chouhan, A.K., Bengali, E., Romero-Oetega, M.I. Modality-Specific Axonal Regeneration: Toward Selective Regenerative Neural Interfaces. Front Neuroengineering. 2011. 4: 11

Makwana, M., Werner, A., Acosta-Saltos, A., Gonitel, R., Pararajasingham, A., Ruff, C., Rumajogee, P., Cuthill, D., Galiano, M., Bohatschek, M., Wallace, A.S., Anderson, P.N., Mayer, U., Behrens, A., and Raivich, G. Peripheral facial nerve axotomy in mice causes sprouting of motor axons into perineuronal central white matter : time course and molecular characterization. J. Comp. Neurol. 2010. 518: 699–721

Mandolesi, G., Madeddu, F., Bozzi, Y., Maffei, L., Ratto, G.M. Acute physiological response of mammalian central neurons to axotomy: ionic regulation and electrical activity. FASEB J. 2004. 18: 1934–1936

Marasco, P.D., Schultz, A.E., Kuiken, T.A. Sensory capacity of reinnervated skin after redirection of amputated upper limb nerves to the chest. Brain. 2009. 132(6): 1441–1448

- McNaughton, T. G., Horch, K. W. Metallized polymer fibers as leadwires and intrafascicular microelectrodes. *J Neurosci Methods*. 1996. 70:103–110.
- Micera, S., Citi, L. Rigosa, J., Carpaneto, J., Raspopovic, S., Pino, G.D., Rossini, L., Yoshida, K., Denaro, L., Dario, P., Rossini, P.M. Decoding Information From Neural Signals Recorded Using Intra-neural Electrodes: Toward the Development of a Neurocontrolled Hand Prosthesis. *Proceedings of the IEEE*. 2010. 98 (3): 407-417
- Michaevlevski, I., Medzihradzsky, K.F., Lynn, A., Burlingame, A.L., Fainzilber, M. Axonal transport proteomics reveals mobilization of translation machinery to the lesion site in injured sciatic nerve. *Mol Cell Proteomics*. 2010. 9: 976–987
- Miller, L. A., Stubblefield, K. A., Lipschutz, R. D., Lock, B. A. & Kuiken, T. A. Improved myoelectric prosthesis control using targeted reinnervation surgery: a case series. *Neural Systems and Rehabilitation Engineering, IEEE Transactions*. 2008. 16:46-50.
- Molteni, R., Zheng, J.Q., Ying, Z., Gomez-Pinilla, F., Twiss, J.L., Voluntary exercise increases axonal regeneration from sensory neurons. *Proc. Natl. Acad. Sci. U. S.A.* 2004. 101: 8473–8478.
- Mueller, B.K. Growth cone guidance: first steps towards a deeper understanding. *Annual Review of Neuroscience*. 1999. 22, 351–388
- Mukhopadhyay, G., Doherty, P., Walsh, F.S., Crocker, P.R., Filbin, M.T. A novel role for myelin-associated glycoprotein as an inhibitor of axonal regeneration. *Neuron*. 1994. 13 (3), 757–767
- Nakagomi, S., Suzuki, Y., Namikawa, K., Kiryu-Seo, S., and Kiyama, H. Expression of the activating transcription factor-3 prevents c-Jun N-terminal kinase-induced neuronal death by promoting heat shock protein27 expression and Akt activation. *J. Neuroscience*. 2003. 23: 5187–5196
- Navarro, X., Krueger, T. B., Lago, N., Micera, S., Stieglitz, T., Dario, P. A critical review of interfaces with the peripheral nervous system for the control of neuroprostheses and hybrid bionic systems. *Journal of the Peripheral Nervous System*. 2005. 10:229–258
- Navarro, X., Vivo, M., Valero-Cabre, A. Neural plasticity after peripheral nerve injury and regeneration. *Progress in Neurobiology*. 2007. 82: 163–201
- Neri, T., Cregg, J. New Prosthetic arms provide greater quality of life for amputees. Eighth Annual Freshman Conference. Conference Session C9. 2008
- Neumann, S., Skinner, K. Basbaum, A.I. Sustaining intrinsic growth capacity of adult neurons promotes spinal cord regeneration. *PNAS*. 2005. 102 (46)

- Oskoei, M. A. and Hu, H. Myoelectric control systems—A survey. *Biomedical Signal Processing and Control*. 2007. 2(4): 275-294
- Owings, M. F., and Kozak, L. J. Ambulatory and inpatient procedures in the United States, 1996. *Vital Health Stat*. 13, 1998, 1–119
- Patodia, S. and Raivich, G. Downstream effector molecules in successful peripheral nerve regeneration. *Cell Tissue Res*. 2012. 349: 15–26.
- Patodia S, Raivich G. Role of transcription factors in peripheral nerve regeneration. *Front Mol Neuroscience*. 2012. 5:8
- Pfister, L. A., Christen, T., Merkle, H.P., Papaloizos, M. and Gander, B. Novel Biodegradable Nerve Conduits for Peripheral Nerve Regeneration. *European Cells and Materials*. 2004. 7(2): 16-17.
- Raivich, G., Hellweg, R., Kreutzberg, G.W. NGF receptor-mediated reduction in axonal NGF uptake and retrograde transport following sciatic nerve injury and during regeneration. *Neuron*. 1991. 7: 151–164
- Raivich, G., Bohatschek, M., Da Costa, C., Iwata, O., Galiano, M., Hris- tova, M., Nateri, A. S., Makwana, M., Riera-Sans, L., Wolfer, D. P., Lipp, H. P., Aguzzi, A., Wagner, E. F., and Behrens, A. The AP-1 transcription factor c-Jun is required for efficient axonal regeneration. 2004. *Neuron*. 43: 57–67
- Raivich, G. c-Jun activation and function in neural cell death, inflammation and repair. *Journal of Neurochemistry*. 2008. 107: 898-906.
- Ramachandran, A., Schuettler, M., Lago, N., Doerge, T., Koch, K.P., Navarro, X., Hoffmann, K.P, and Stieglitz, T. Design, in vitro and in vivo assessment of a multi-channel sieve electrode with integrated multiplexer. *J. Neural Engineering*. 2006. 3: 114–124
- Rishal, I. and Fainzilbe, M. Retrograde signaling in axonal regeneration. *Experimental Neurology*. 2010. 223 (1): 5-10
- Saito, H and Dahlin, L. B. Expression of ATF3 and axonal outgrowth are impaired after delayed nerve repair. *BMC Neuroscience*. 2008. 9 (88): 1-10
- Seifert, J.L., Desai, V., Watson, R.C., Musa, T., Kim, Y., Keefer, E.W., and Romero, M.I. Normal Molecular Repair Mechanisms in Regenerative Peripheral Nerve Interfaces Allow Recording of Early Spike Activity Despite Immature Myelination. *IEEE Transactions on neural systems and Rehabilitation Engineering*. 2012. 20 (2): 220-227

Seiffers, R., Allchorne, A.J., Woolf, C.J. The transcription factor ATF-3 promotes neurite outgrowth. *Mol Cell Neuroscience*. 2006. 32:143-154

Seiffers, R., Mills, C. D. and Woolf, C. J. ATF3 Increases the Intrinsic Growth State of DRG Neurons to Enhance Peripheral Nerve Regeneration. *Cellular / Molecular*. 2007. *The Journal of Neuroscience*. 2007. 27(30):7911–7920

Simeral, J., Kim, S., Black, M., Donoghue, J. & Hochberg, L. Neural control of cursor trajectory and click by a human with tetraplegia 1000 days after implant of an intracortical microelectrode array. *Journal of Neural Engineering* 8. 2011.

Soechting, J. F. and Flanders M. Flexibility and Repeatability of Finger Movements during Typing: Analysis of Multiple Degrees of Freedom. *Journal of Computational Neuroscience*. 1997. 4: 29–46

Stoll, G., Griffin, J.W., Li, C.Y., Trapp, B.D.: Wallerian degeneration in the peripheral nervous system: participation of both Schwann cells and macrophages in myelin degradation. *J Neurocytol* 1989, 18:671-683

Stoll, G., and Müller, H. W. Nerve Injury, Axonal Degeneration and Neural Regeneration: Basic Insights. *Brain Pathology*. 1999. 9: 313-325

Suner, S., Fellows, M.R., Vargas-Irwin, C., Nakata, G.K., Donoghue, J.P. Reliability of signals from a chronically implanted, silicon-based electrode array in non-human primate primary motor cortex. *IEEE Transactions Neural System Rehabilitation Engineer*. 2005. 13 (4): 523-541

Taylor Z and Miller K. Reassessment of brain elasticity for analysis of biomechanisms of hydrocephalus. *Journal of Biomechanics*. 2004. 37(8): 1263-1269

Thelin, J. Jorntell, H., Psouni, E., Garwicz, M., Schouenborg, J., Danielsen, N., Linsmeier, C.E. Implant Size and Fixation Mode Strongly Influence Tissue Reactions in the CNS. *PLoS ONE*. 2011. 6(1)

Thurston, A. J. Pare´ and prosthetics: the early history of artificial limbs. *ANZ J. Surg*. 2007. 77: 1114–1119

Tofaris, G.K., Patterson, P.H., Jessen, K.R., Mirsky, R. Denervated Schwann cells attract macrophages by secretion of leukemia inhibitory factor (LIF) and monocyte chemoattractant protein-1 in a process regulated by interleukin-6 and LIF. *J. Neuroscience*. 2002. 22, 6696–6703

Touch Bionics. Active prosthetic: i-Limb Digits & Living skin. 2012

Trapp, B.D., Hauer, P., Lemke, G. Axonal regulation of myelin protein mRNA levels in actively myelinating Schwann cells. *J Neuroscience*. 1988. 8:3515-3521

Tyler, D.J., Durand, D. M. Functionally selective peripheral nerve stimulation with a flat interface nerve electrode. *IEEE Trans Neural Syst Rehabil Eng.* 2002. 10:294–303

Tsujino, H., Kondo, E., Fukuoka, T., Dai, Y., Tokunaga, A., Miki, K., Yonenobu, K., Ochi, T., Noguchi, K. Activating transcription factor 3 (ATF3) induction by axotomy in sensory and motoneurons: A novel neuronal marker of nerve injury. *Mol Cell Neuroscience.* 2000. 15:170-182

Udina, E., Cobianchi, S., Allodi, I, Navarro, X. Effects of activity-dependent strategies on regeneration and plasticity after peripheral nerve injuries. *Annals of Anatomy.* 2011. 193: 347-353

Udina, E. Puigdemasa, A., Navarro, X. Passive and Active exercise improve regeneration and muscle reinnervation after peripheral nerve injury in rat. *Muscle & Nerve.* 2011

Waller, A. Experiments on the section of the glossopharyngeal and hypoglossal nerves of the frog, and observations of the alterations produced thereby in the structure of their primitive fibers. *Philos. Trans. R. Soc. London (Biol.).* 1850. 140: 423-429

Watson, C.R. Investigations into causes of failure of regenerative peripheral nerve interfaces. 2012.

Watson, W.E. The binding of actinomycin D to the nuclei of axotomized neurons. *Brain Res.* 1974. 65 (1974), pp. 317–322

Williams, J. C., Hippensteel, J. A., and Dilgen, J. et al. Complex impedance spectroscopy for monitoring tissue responses to inserted neural implants. *J. Neural Eng.* 2007. 4(4): 410–423,

Wilton, D., Arthur-Farraj, P., Latouche, M., Turmaine, M., Behrens, A., Mirsky, R., Raivich, G., and Jessen, K. Schwann cell c-Jun is essential for peripheral nerve regeneration. 2009. *Glia.* 57: S158

Yoshida, K., Horch K. Selective stimulation of peripheral nerve fibers using dual intrafascicular electrodes. *IEEE Trans Biomed Eng.* 1993. 40 (5):492–494

Ziegler-Graham, K., MacKenzie, E. J., Ephraim, P. L., Trivison, T. G. and Brookmeyer, R. Estimating the prevalence of limb loss in the United States: 2005 to 2050. *Archives of physical medicine and rehabilitation.* 2008. 89: 422-429

Zuo, J., Neubauer, D., Graham, J., Krekoski, C.A., Ferguson, T.A., Muir, D. Regeneration of axons after nerve transection repair is enhanced by degradation of chondroitin sulfate proteoglycan. *Experimental Neurology.* 2002. 176 (1), 221–228

BIOGRAPHICAL INFORMATION

Sarita Bhetawal has received her Bachelor degree in Biochemistry / Biotechnology from Minnesota State University, Mankato in summer, 2009. She was an intern at R & D Systems, Minneapolis MN, in summer of 2007 and at Genmab, Brooklyn Park MN, in summer, 2008. She began her Graduate studies in Bioengineering at University of Texas, Arlington in fall, 2010. She joined Regenerative Neurobiology laboratory under the mentorship of Dr. Mario I. Romero-Ortega in fall, 2010 and worked as a Graduate Research Assistant since spring, 2011.